IEEE Access
Multidisciplinary | Rapid Review | Open Access Journal

Received 2 June 2023, accepted 20 June 2023, date of publication 30 June 2023, date of current version 6 July 2023.

Digital Object Identifier 10.1109/ACCESS.2023.3291009

RESEARCH ARTICLE

Enhancing Dynamic Voltage Stability in Resilient Microgrids Using FACTS Devices

LUIS A. PAREDES, (Member, IEEE), MARCELO G. MOLINA, (Senior Member, IEEE), AND BENJAMÍN R. SERRANO

Institute of Electrical Energy, Universidad Nacional de San Juan—CONICET, San Juan 5400, Argentina

Corresponding author: Luis A. Paredes (lparedes@ieee.org)

This work was supported in part by the German Academic Exchange Service (DAAD), and in part by the National Council for Scientific and Technical Research of Argentina (CONICET).

ABSTRACT Microgrids (MGs) have emerged throughout the world as the major means of integrating a variety of distributed energy resource (DER) technologies into the distribution system. These DER technologies are mostly coupled through electronic power converters (EPCs). This fact has created new operation challenges as these converter-interfaced DERs could compromise the MG stability, reliability, and resilience margins. On the other hand, induction motor-type loads (IMs) are dynamic loads with the greatest incidence in distribution grids. Air conditioning (A/C) type loads have IMs among their components. IMs demand considerable amounts of reactive power for their correct operation. In particular, when there are disturbances in MGs with high penetration of these types of loads, the phenomenon of fault-induced delay voltage recovery (FIDVR) occurs. This phenomenon causes problems with the dynamic voltage stability (DVS) due to the deficit and inability to supply reactive power of the DERs generator park composing the MG, which could lead to a voltage collapse. To face these new issues, this work proposes an approach to incorporate flexible ac transmission system (FACTS) controllers, such as an SVC and a DSTATCOM, into the grid as reactive power supply resources for improving the microgrid dynamic voltage stability. The proposal includes the design, optimal location, and dynamic modeling of FACTS devices aiming at enhancing MG operation resilience. For validation of the developed methodology, an MG test system reported in the literature and a real microgrid system of the Galapagos Islands in Ecuador have been used. The results demonstrated the superiority of DSTATCOM over SVC in enhancing DVS, FIDVR mitigation, and consequently operational resilience.

INDEX TERMS Dynamic voltage stability, FACTS, SVC, DSTATCOM, resilient microgrids.

NOMENCLATURE

Abbreviations

MG	Microgrid.
DER	Distributed energy resources.
EPC	Electronic power converter.
IM	Induction motor-type loads.
A/C	Air conditioning.
FIDVR	Fault-induced delay voltage recovery.
DVS	Dynamic voltage stability.
FACTS	Flexible ac transmission system.
VAr	Volt ampere reactive.
SVC	Static VAr compensator.
DSTATCOM	Distribution static compensator.
WP	Wind power.
PV	Solar photovoltaic.
DVI	Dynamic voltage instability.
LVRT	Low voltage ride through.
PCC	Point of common coupling.
P-Q	An exponential polynomial model of active and reactive power of static loads.
GTO	Semiconductor elements gate turn-off.
IGBT	Insulated gate bipolar transistors.
PWM	Pulse-width modulation.
ZIP	Static loads modeled from impedances, current and constant powers.

The associate editor coordinating the review of this manuscript and approving it for publication was Fei Gao.

WF	Without FACTS.
SC1,2,3,4	Operating scenarios: 1,2,3,4.
SG	Synchronous generation.
Sce $\mathbb{R}$	Resilient scenario.
BAL	Baltra.
SCR	Santa Cruz.
SC	Event of short-circuits.
Symbols	
DVI_j^k	Voltage deviation index where j and k are the types of faults and FACTS devices node location in the MG.
$DVPI_j^k$	Dynamic voltage performance index where j and k are the types of faults and FACTS devices node location in the MG.
$TDVSI_j^k$	Transient dynamic voltage severity index where j and k are the types of faults and FACTS devices node location in the MG.
P_e	Electrical power demanded by the IM disregarding stator losses.
H_m	Constant inertia of the IM.
P_m	Mechanical load applied to the IM.
k_{put}	Gain for the P is calculated as a function of the supply and reference voltages.
k_{qut}	Gain for the Q is calculated as a function of the supply and reference voltages.
$A \sim Poi\left(\lambda_1\right)$	Contingency N–1 of disconnection of the MG feeder in a Poisson distribution where λ_1 is to the historical failure percent.
$\mathbb{R}$	Represents the probability of success for the double simultaneous contingencies.
$\mathbb{E}\left[A+B\right]_{Scei}$	Mathematical expectation for each resilient contingency scenario *Scei* based on probabilistic resilience approach $\mathbb{R}$ and the DVS analysis.
ΔI_q	Relative amount of capacitive (+Q) or inductive (–Q) current injected by the DER.
ΔV_f	Relative change in the PCC voltage during the fault.
I_q	Injection reactive current reference q frame qd of inverter DER.
I_d	Injection reactive current reference d frame qd of inverter DER.
k	Proportional scaling factor current of inverter DER.

I. INTRODUCTION

The decarbonization needs of the global electricity matrix, the growing increase in distributed energy resources (DERs) based on non-conventional renewable energies such as wind power (WP) and solar photovoltaic (PV), together with the difficulties of access to electricity in remote communities have given rise to a new energy infrastructure paradigm called Microgrid (MG). MGs facilitate access and universality to electrical energy, and because of their inherent characteristics, they allow the integration of different DER technologies, as well as different types of static and dynamic loads (also called fixed and flexible loads, respectively) [1]. From the operation point of view, MGs can operate in two modes: connected to a distribution network or in isolated/autonomous operation mode [2]. The control schemes that govern the MGs are categorized into three levels or layers with different scopes of applicability: (i) primary control, coordinating the local control operation for each DER, and loads in the MG. It is based on the local measurements of those parameters necessary for managing, operating, and controlling the MG in fast perturbations; (ii) secondary control responsible for MG operation according to the mode of operation used, and (iii) tertiary control, which is the highest control level and associates the operation in terms of economic dispatch. It can also coordinate multiple MGs interacting with each other in a system, communicating requirements from the distribution network in a cluster of MGs [3].

The high penetration of PV and WP DERs electrically coupled to the MG through electronic power converters (EPCs) may cause dynamic voltage instability (DVI) scenarios when the control schemes of these devices do not have Low Voltage Ride Through (LVRT) features or support operating schemes which may allow dynamic voltage control. In comparison, when DERs are based on synchronous generation, their reactive power supply capacities are limited due to their capacity curve and their excitation systems which may lead to voltage instability problems, especially in isolated MGs [4]. Concerning the load components, these can also cause problems with voltage control and stability in MGs. The massive connection of induction motors (IMs) represents a threat to dynamic voltage stability (DVS) when disturbances occur due to the deceleration and possible blocking of the IMs. These problems are the leading cause of the fault-induced delay voltage recovery (FIDVR) phenomenon and in extreme situations may lead to prolonged voltage instabilities and rapid collapses [5]. The massive penetration of air conditioners (A/Cs) in recent years has been constantly increasing. These are dynamic loads by nature because their main components have one or more induction motors. The modeling of this type of dynamic load plays a crucial role when analyzing the occurrence of FIDVR events or, in turn, DVI [6]. The flexible ac transmission systems (FACTS) technology has enabled the mitigation of critical problems related to the stability of bulk electric power systems. However, with the recent growth and positioning of MGs, new and different problems associated with voltage stability have arisen.

Based on the above, this paper proposes the incorporation of SVC (static VAr compensator) and DSTATCOM (distribution static compensator) type FACTS devices as reactive power supply resources for improving and mitigating problems associated with dynamic voltage stability in microgrids. To this aim, the dynamic performance of these devices is comparatively analyzed, including the improvements achieved in the operation resilience of MGs, which FACTS technology

can provide, operating in a coordinated mode with the DERs. In this sense, the work presents the main investigations in the literature that address the incorporation of FACTS devices in MG, considering different approaches. However, most of them have focused solely on the analysis of N-1 type contingencies, which constitutes a limitation when it comes to analyzing and studying the operational resilience of microgrids threatened by the occurrence of resilient contingencies. Resilient contingencies are those that have a low probability of occurrence in the power system but cause high operational impacts that in most cases generate various types of instabilities. In MGs, simultaneous contingencies of the type are considered resilient due to the detrimental impacts they can cause when they occur. Due to their operational nature, MGs must be designed and planned to perform resiliently from an infrastructure and operational standpoint.

The model of the electronic power converters associated with DERs technologies is performed with LVRT schemes, considering the reactive power support requirements in the presence of resilient disturbances. In addition, they fulfill the normative guidelines of the IEEE-1547-2018 standard. For the application of the developed methodology, a microgrid test system reported in the literature and a real microgrid system of the Galapagos Islands in Ecuador is considered. Dynamic loads of IM type and static loads modeled at constant powers are considered in different percentage penetrations for the case of the test microgrid. For the demand of the Galapagos Islands MG, it has been analyzed detailed modeling of A/C, which showed the difficulties to maintain DVS in contingency situations with a large amount of A/C connected. To analyze the improvements in terms of the MG operational resilience, a probabilistic model of disturbance analysis using a Poisson distribution technique was considered. Improvements in DVS resilience of the MG and mitigation of FIDVR were carried out through simulations in the time domain and with the calculation of indices and metrics which correlate both variables mentioned. Regarding the optimal location of FACTS technologies in MGs, an optimization algorithm developed in a Python environment allowing the achievement of this objective is proposed. The paper ends with a comparative analysis based on the dynamic voltage performance between the two devices i.e., DSTATCOM and SVC.

A. LITERATURE REVIEW

A literary review of the works and research that have been carried out in different areas related to this work is presented here. Firstly, the importance of modeling and load behavior in MGs to identify and solve associated problems is addressed. Residential air conditioning (A/C) loads have among their main components induction motors (IMs), which are generally low inertia machines that make electrical systems more vulnerable to short-term dynamic voltage instabilities under the presence of disturbances. Additionally, some studies have been reported in the literature to analyze the problems of loads in MG systems, which are mentioned below. The study presented in [7] shows several models of dynamic loads in an MG. It shows that when unscheduled transitions of the MG to its island mode occur, depending on the dynamic load component, there are scenarios that present problems with voltage and frequency stability. In the same way, researchers in [8] examine the problem of voltage stability in a low-voltage distribution network. The electrical system in this work has IMs-type loads, for which they propose a dynamic model of a PV inverter operating with 3 control strategies, to provide dynamic voltage support. This allows for avoiding DVI in simple contingencies and with different levels of penetration of PV generation in the distribution network.

Several DVI mitigation techniques have been proposed in the literature in case of contingencies. From these, those that propose load shedding and disconnection schemes stand out. For instance, in [9] it is described that the multiple connections of IMs cause voltage stability problems due to the relationship of dynamic coupling between the change of the IMs and the voltage supply of the system. As a possible solution to this problem, it is suggested to gradually disconnect the IMs that make up the MG. However, these techniques are not considered in this research because load shedding contradicts the operational resilience capacity of MGs. In [10], a distributed voltage control scheme was proposed to supply reactive power through the inverters in stand-alone MGs with static loads; being this a vital study in this topic. However, the limitation of this work is that only steady-state voltage stability is addressed. On the other hand, the study presented in [11] shows a microgrid system adapted from the IEEE 4-bus system composed of a diesel generator and a photovoltaic system to dynamically support the voltage through a control algorithm. The disturbances to which the MG system is subjected are slight and therefore it shows good behavior in terms of voltage stability. In comparison, the analyzed contingencies are not resilient, and the considered load model is only of industrial type. Another technique considered to improve DVS is the incorporation of reactive power compensation devices based on power electronics equipment, particularly FACTS [12]. Implementing this type of technology brings with it multiple benefits to improve the operability of microgrids to avoid load shedding, improve stability margins, and suitably fit the operational requirements of the MG to enhance its resilience [13], [14].

Among the FACTS devices, SVC and DSTATCOM/STATCOM stand out due to their fast-operating response to compensate for reactive power, improve voltage stability in dynamic and static states, avoid dynamic voltage oscillations, and control the voltage module. In this sense, some reported works that have considered the incorporation of these devices have been analyzed. In [15], the incorporation of 3 SVC units in the presence of short circuits in a part of the electrical power system of Saudi Arabia is utilized to improve performance and prevent voltage collapse. Additionally, the improvements in the operational performance of the IMs with the operation of the SVC devices in such short-circuit situations are included. In [16] a dynamic

optimization technique was used to obtain the optimal location and sizing of SVC devices in a real system in the USA, with the presence of A/C load characteristics, to improve the dynamic voltage performance under a large disturbance. Similarly, in [17] a day and night control algorithm was proposed for active and reactive powers in a bulk test power system made up of conventional generation, PV, and a STATCOM device to mitigate FIDVR that meets and exceeds satisfactorily the requirements of the German network code. In [18], reactive power and voltage stability performance in the incorporation of an SVC and STATCOM in an MG test system that has a doubly fed induction generator (DFIG)-based wind farm was comparatively analyzed. In the study developed, a sensitivity index was proposed by which a STATCOM can be located in a distribution system, whose objective is to improve the voltage profile for the maximum use of the DER in case of single-phase faults [19]. The research in [20] focused on improvements to power quality particularly voltage control, harmonic distortion, reactive power compensation, and power factor in an isolated MG through the use of a DSTATCOM and an adaptive switched filter compensator type D-FACTS. In the same way, in [21] researchers dealt with a multi-objective approach to program MGs operation incorporating a DSTATCOM to improve reactive power management and mitigate over and under voltages. In the study [22], an MG interconnected to a distribution network incorporates a STATCOM to regulate the exchange of reactive power flow and control the voltage at the point of common coupling (PCC). As is well known, the massive presence of wind generation in an electrical system brings problems to the DVS. Due to this, in [23] a STATCOM has been incorporated that operates in coordination with the WP equipped with an LVRT system in different operating conditions. In addition, an evaluation and improvement analysis of DVS is presented in [24], which is focused on the impact of including a DSTATCOM in an MG with high IM-type dynamic load penetration when a fault occurs causing the microgrid isolation.

Similarly, in [25] an LVRT scheme is investigated in a coordinated operating environment interconnecting the MG to a distribution network, with the implementation of a DSTATCOM in different locations, for reactive power support during the occurrence of external faults. Another approach is shown in [26], where the incorporation of smart inverters associated with PV DERs is explored to maximize FIDVR according to the variation of solar radiation in several test distribution systems. Researchers in [27] proposed the incorporation of a DSTATCOM and smart inverters associated with PV generation. This development scheme improves the dynamic voltage support and includes an economic evaluation to incorporate the DSTATCOM in an isolated MG. In [28], a methodology for optimal placement of DSTATCOM-type devices is proposed, whose primary focus is to improve the steady-state voltage profile and the voltage unbalance between phases of low voltage networks. The article in [29] proposes the incorporation of a STATCOM in an MG to satisfy reactive power needs, whose primary focus is the simulation of disturbances based on step load changes to understand and improve the voltage profile in the MG, limiting the study to the analysis of short-circuit type disturbances or resilient contingencies. In [30], an MG system based on the IEEE 9-bus model is adapted, where the voltage stability is improved through an SVC and the transient stability with a coordinated SVC-PS device in the face of three-phase 6-cycle faults. In [31], a collaborative control between an SVC and DSTATCOM is presented in a DC MG connected to an electric grid, where the SVC is employed for supplying the steady state reactive power needs while the DSTATCOM improves the dynamic voltage conditions and flicker and power factor reduction.

The authors in [32] proposed an intelligent fuzzy control that allowed improving voltage stability and power quality through a DSTATCOM, respectively, in a hybrid AC/DC MG. On the other hand, in [33], an interesting analysis of voltage stability in hybrid AC/DC MGs is addressed; which with the help of a droop controller improves transient and voltage stability. An important study that relates the response and operational contribution of including a STATCOM in a small-scale MG is presented in [34], where the optimal adjustment of the STATCOM parameters allows controlling and regulating the voltage and frequency oscillations in the event of simple short-circuit faults in the PCC.

On the other hand, works presented in [35] and [36] propose the resilient operation improvement of an MG to avoid a blackout in case of an event that causes its isolation. This study stands out since through dynamic optimization they establish the requirements of the DERs units from the standpoint of planning to supply the demand before the hourly presence of a fault associated with DVS and frequency restrictions. Lastly, at present, new control strategies based on dual-stage fractional order PID and utilizing an imperialist competitive algorithm for the analysis of interconnected microgrids as a single entity in autonomous mode offer important improvements for primary frequency and stability regulation, which are promising solutions to address future improvements in microgrid resilience [37]. In addition, to improve the power quality and frequency stability of hybrid systems including numerous energy sources, the proposal to use a fuzzy tilt integral derivative (FTID) with a filter plus double integral (FTIDF-II) control strategy for frequency control in microgrids is presented in [38]. In this study, the results obtained are better than the classical techniques of frequency regulation, which foresees new trends in these issues that can be scaled for the analysis of the operational resilience of hybrid power systems [38]. In the work proposed in [39], it is presented an interesting dynamic control mechanism of voltage source converter type DERs. It is also used for hybrid generation systems (WP and PV) including a current source converter topology added to a supercapacitor for smoothing the voltage ripple in the converter and therefore the harmonics

content in the distribution network. This research represents novel control mechanisms of applicability to microgrid systems.

B. PROBLEM IDENTIFICATION

Based on the bibliographical review carried out, it is evident that there is a lack of significant contributions regarding the evaluation of dynamic voltage stability analysis in microgrid systems experiencing simultaneous contingencies of resilient nature. These contingencies, although having a low probability of occurrence, can have significant operational impacts. Furthermore, while international grid codes and the IEEE-1547-2018 standard permit power electronic converters associated with DERs in MGs to operate in smart mode, there remains a considerable deficit of reactive power when this type of generation is affected by resilient faults. This deficit hinders the ability to maintain stability and operability of the system, particularly with high penetration of dynamic loads. Moreover, there is a notable absence of a comparative analysis regarding the utilization of FACTS devices in shunt connection to address these DVS and resilience issues in MGs. Consequently, no metric or index has been developed to quantitatively evaluate a resilient event of type N-1-1, thereby quantifying the operational resilience of electrical microgrids following contingencies. As a result, there exists a significant gap in addressing the close relationship between dynamic voltage stability and operational resilience in electrical microgrids.

C. CONTRIBUTIONS

Based on the identified gaps and deficiencies, this paper aims to address the following aspects:

1) The analysis of dynamic voltage stability in MG systems during operational isolation resulting from contingencies of resilient characteristics. Two MG test systems with different topological characteristics are taken into consideration to validate the developed methodology. The first is a new MG system reported in the literature [40], which is characterized by having feeders composed of insulated underground cables and with a predominant presence of renewable DERs based on solar PV and wind types. The second system corresponds to a real MG located in the Galapagos Islands in Ecuador. This microgrid has been modeled and parameterized according to its real operating behavior, to reproduce its drawbacks associated with dynamic voltage instability in the presence of severe contingencies. In terms of infrastructure, this microgrid stands out due to its combination of aerial, underground, and submarine feeders. Additionally, it exhibits a diverse range of DER technologies and storage systems.
2) The dynamic modeling of several types of loads, including induction motors, air conditioners, and hybrid schemes with static loads (through an exponential P-Q polynomial model) and dynamic loads (IMs+A/C). This is done to demonstrate and reproduce the inconveniences that these types of loads cause in the voltage dynamic behavior when they are connected to the microgrid systems addressed.
3) The improvements to the DVS in the MGs analyzed are achieved with the incorporation of two FACTS devices: SVC and DSTATCOM that are introduced and operated separately but under a primary centralized coordinated control scheme with the DERs that make up each MG. Additionally, a comparative analysis is carried out based on the dynamic performance of FACTS devices to determine which response is better in terms of DVS.
4) The optimal siting of FACTS connections within the microgrid. To achieve this, an optimization problem is formulated and solved, taking into consideration performance indices that are directly related to the dynamic behavior of voltage. This approach allows for the identification of the most suitable locations within the microgrid to install FACTS devices, maximizing their effectiveness in improving dynamic voltage stability.
5) To conclude, the evaluation of resilient-type contingencies in microgrids. To achieve this, a novel evaluation metric is proposed which allows for the correlation between dynamic voltage stability and the operational resilience of the microgrid. This metric provides a means to assess the impact of contingencies on both the dynamic voltage stability and the overall resilience of the microgrid system.

The rest of the paper is organized as follows. The dynamic voltage stability, evaluation indices, its normative characterization, load modeling, and the FIDVR phenomenon are presented in Section II. Subsequently, in section III, a quantitative metric of probabilistic evaluation of resilience is included. Then, FACTS devices and smart inverters modeled are exposed in section IV. In section V, case studies are conducted using two test systems. The results obtained from these studies, along with comparative analyses between FACTS devices and their optimal placement, are presented. Next, in Section VI, the discussion obtained from the work is developed. Finally, in Section VII, the paper concludes with a summary of the findings and their implications.

II. DYNAMIC VOLTAGE STABILITY ANALYSIS

In traditional electrical power systems, synchronous machines are the predominant generation systems. These machines have well-defined controllers that effectively regulate the active and reactive power flows under normal and contingency conditions. An intrinsic characteristic of synchronous generators is their heavy rotor, which provides significant inertia for avoiding instabilities caused by sudden changes in rotor speed during disturbances. However, DERs integrated into microgrid systems through electronic power converters lack inherent inertia due to their construction characteristics. As a result, control strategies and algorithms

have been developed to provide virtual inertia, enabling control and management of active and reactive power. Nevertheless, these DERs face limitations associated with the intermittent nature of their primary energy sources, either solar radiation or wind in the case of the PV and WP generations, respectively. When DERs integrated through EPCs constitute the majority of generation in a microgrid, the challenges related to maintaining dynamic voltage stability become more complex during microgrid isolation. This is primarily due to the deficit in supplying reactive power, which is essential for maintaining system operability. Therefore, DERs must be equipped with support and dynamic control schemes that enable the provision of reactive power during fault conditions, intending to secure the operability of the MG, ensuring the stability and reliable operation of the microgrid [41].

Dynamic voltage stability in microgrids can be defined as the system's ability to restore its permissible operating voltage level within a short timeframe after the occurrence of contingencies (or disturbances). In particular, the DVS also called short-term voltage stability is an analysis that is conducted in the time domain framework, focusing on a short-range scale typically up to 5s [42]. Additionally, to analyze the dynamic voltage stability, it is crucial to accurately model the dynamic behavior of loads. Similarly, when considering short-duration faults located in close proximity to loads, understanding their impact on the microgrid's performance and dynamic response becomes a primary concern. Furthermore, the relationship between the dynamic voltage stability (DVS) and the hierarchical controllability scheme of the microgrid is significant. This scheme encompasses the coordinated primary control system among DERs components and FACTS devices [43]. This coordination plays a pivotal role in the analysis of the microgrid operational resilience, representing a critical aspect to be addressed.

Generally, to analyze the DVS, voltage-time type signals are commonly used to visualize the operational dynamic response of these variables when the MG is subjected to disturbances. On the other hand, to mathematically quantify the dynamic performance of the voltage, different indices are introduced to achieve this objective, as shown below.

A. PERFORMANCE INDICES FOR DYNAMIC VOLTAGE STABILITY ANALYSIS IN MICROGRIDS

1) VOLTAGE DEVIATION INDEX (VDI)

This index relates the deviation of the voltage module i of the discretized signal at instant t concerning the voltage module in pre-fault conditions, which has been considered to be 1.0 p.u. Expression (1) shows the mathematical calculation relationship for this index [21]. It is necessary to clarify that, if the DVI_j^k is closer to 0 p.u., this will represent better post-disturbance voltage performance; otherwise, when it is closer to 1.0 p.u., it indicates poor dynamic voltage performance and it can be interpreted as a dynamic voltage instability scenario.

$$DVI_j^k = \sum_{V_i \in \beta} \sum_{t \in T} \frac{|1.0 - V_{i,t}|}{N_N \cdot N_S} \quad \forall V_i \in [\beta] \wedge \forall t \in [T] \tag{1}$$

where j and k are the types of faults and FACTS devices node location in the MG, respectively. V_i represents the voltage magnitude in the sample space $\boldsymbol{\beta}$ of the voltages to the simulation signal for time t_i, and N_N is the number of nodes and N_S is the number of samples in the discretized signal.

2) DYNAMIC VOLTAGE PERFORMANCE INDEX (DVPI)

Ideally, the voltage behavior as a function of time when there is no fault in the MG shows a voltage level close to 1.0 p.u. at all times. A different situation occurs when the system is subjected to a disturbance. In that case, the transient dynamics of the process causes distortions in the system voltage. The analysis carried out to determine the dynamic voltage performance index (DVPI) is calculated using (2).

$$DVPI_j^k = \frac{1}{N_N} \sum_{t_i=0}^{T} \sum_{i=1}^{\beta} [\Delta t_i \cdot |V_i|] \quad \forall \Delta t_i \in [0, T] \wedge \forall V_i \in [\beta] \tag{2}$$

where j and k are the types of faults and FACTS devices node location in the MG, respectively. V_i represents the voltage magnitude of the simulation signal for time Δt_i, β represents the total number of discrete voltage magnitude samples in the analyzed time window T, and N_N is the number of nodes. When $DVPI_j^k$ is closer of the pre-fault voltage and the time T, which corresponds to the analyzed time window, the MG has a better performance in terms of dynamic voltage response. For example, for the studies cases of this work, in stable conditions without the presence of faults in the MG and for a time window of 5 s with $\Delta t_i = 0.001$, the DVPI would be equal to 5 (since 0.001· 5000=5).

3) TRANSIENT DYNAMIC VOLTAGE SEVERITY INDEX (TDVSI)

To quantify the voltage dynamic behavior during and after the fault that caused the MG isolation, it is introduced a mathematical expression that allows evaluating and determining the performance in terms of DVS. The transient dynamic voltage severity index (TDVSI) is presented in (3), which was adapted from [44] and modified for the analysis in MGs.

$$TDVSI_j^k = \frac{\sum_{i=1}^{N} \sum_{t=T_d}^{T} \left[\frac{|V_{i,t} - V_{i,0}|}{V_{i,0}} \right]}{N_N \, (T - T_d)} \quad \forall t \in [T_d, T] \tag{3}$$

where j and k are the kind of fault and node location of SVC or DSTATCOM in the MG, respectively. i represents different MG nodes, N_N is the number of nodes. $V_{i,t}$ is the node i voltage magnitude at time t obtained from the dynamic simulation in the time domain, $V_{i,0}$ is the voltage magnitude in pre-fault conditions, T_d and T represent the fault clearance

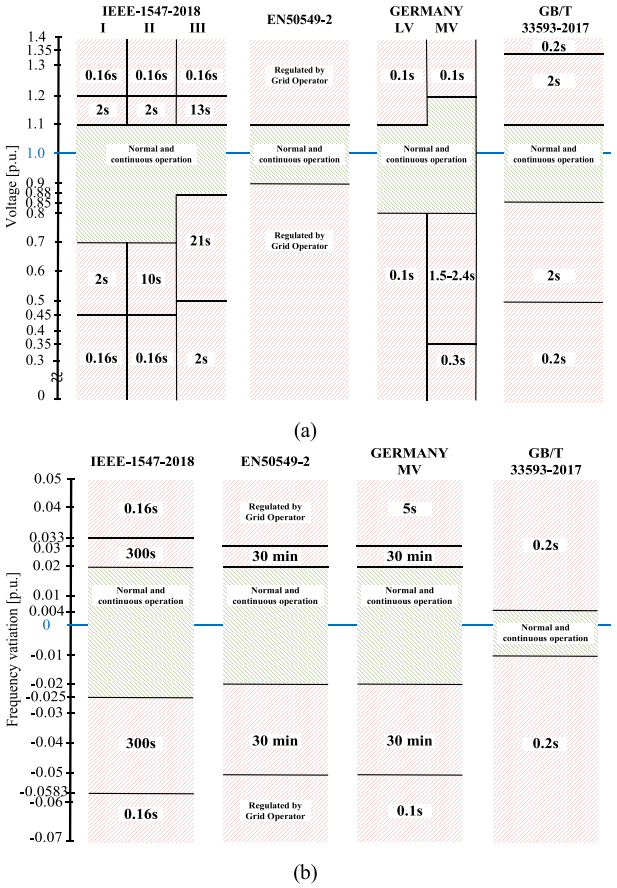

FIGURE 1. Main standards and grid codes that describe the operational requirements for synchronizing DERs in microgrids. (a) Voltage and (b) frequency.

time and the time of the analysis window in the simulation process, respectively. A lower $TDVSI_j^k$ value indicates a better transient voltage performance.

B. MAIN STANDARDS AND GRID CODES RELATED TO VOLTAGE AND FREQUENCY OPERATING REQUIREMENTS FOR SYNCHRONIZATION OF DERS IN MICROGRIDS

Although there is currently no global standard that regulates the network codes for isolated and interconnected microgrid systems, several countries and power system research entities have proposed codes and requirements to be met by DERs units for their operational incorporation into distribution systems with a view to future microgrids to ensure the stability margins both in voltage and frequency. In this sense, the following is a brief description of the permissible values of voltage and frequency magnitudes with their operating times that allow the correct synchronization of DERs to ensure the stability and control of these units in steady-state and under the threat of contingencies. Following are different international standards and regulations: IEEE-1547-2018, CENELEC EN50549-2, and the German and Chinese grid codes. So, in terms of voltage the allowable operating requirements and their associated response times for DERs in the presence of contingencies are shown in Fig. 1. By complying with these response ranges of DER units, it is intended that there will be the operational and response flexibility of the electronic inverter-based units. It is noteworthy the permissibility of the IEEE-1547-2018 standard to low voltages which positions it as the standard with the best applicability in microgrid environments. On the other hand, the other standards presented face very well the LVRT and HVRT conditions in DERs for medium voltage distribution systems. Furthermore, the synchronization and operational response range in terms of the frequency of DER units in distribution systems with a view to possible future inclusion in microgrid systems are presented in Fig. 1(b). The fulfillment of the conditions in frequency magnitude and response time will ensure that the DER inverters respond effectively to secure the operating frequency [45], [46].

C. REGULATORY REQUIREMENTS OF THE IEEE STD 1547-2018 RELATED TO DVS IN MICROGRIDS

LVRT dynamic voltage support is understood as any action aimed at supporting the stability and quality of voltage during disturbances. Generation plants, whether PV or wind, coupled via an electronic inverter, must be able to: i) remain connected during a failure; ii) support the stability and quality of voltage by injecting reactive power during a fault, and iii) consume the same amount or less of reactive power once the fault is cleared [46]. The IEEE Std 1547-2018 states that in the event of any voltage disturbance of any duration, the DER should not de-energize or stop supplying active power flow according to its availability. Its power input must be as large as its pre-level disturbance, prorating it for the minimum voltage level in p.u. if the voltage is better than the rated voltage. Active power deviations lasting no more than 0.5 s will be allowed. DERs must be subjected to the operational requirements established by the standard in the presence of disturbances mainly originated from contingencies. To correlate the quick and effective response of smart inverters to improve the MG operational resilience and mitigate voltage instabilities in the short term, the analysis carried out in this section corresponds to the DERs classified in the standard as Category I (rated power up to 10 MVA). Therefore, the DERs response in terms of their operating voltage must be considered according to the guidelines, operating requirements, and action and response times expressed in accordance with the characteristics of Fig. 2 [47]. The modeling of smart inverters must be done in accordance with what was previously stated, considering the LVRT characteristics, as will be described in section IV.

Load components play a key role in the analysis of the DVS. Therefore, the types of loads considered in the paper will be described below, highlighting static and dynamic loads.

D. DYNAMIC LOADS AND THEIR INFLUENCE ON DVS

1) INDUCTION MOTOR

For studies related to stability, the modeling of dynamic loads, in this case particularly the IMs, must be performed in a

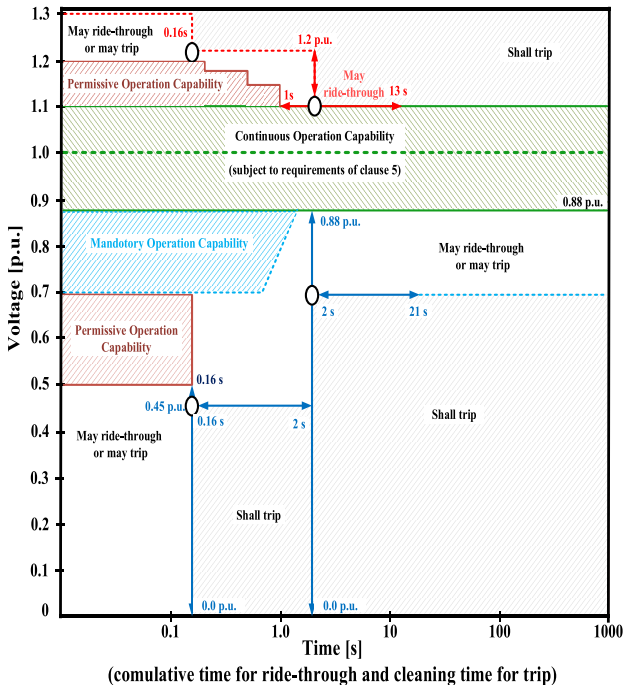

FIGURE 2. DERs response to abnormal operating performance voltages and voltage ride-through requirement for Inverters Category I [32].

way that allows reproducing the dynamic behavior of the IMs under variations that perturb the frequency and voltage. The most typical case of voltage instability in the short term occurs due to the braking of the IMs after the occurrence of a large disturbance. This phenomenon is caused by a loss of equilibrium between electromagnetic and mechanical torques or by the lack of attraction to stable equilibrium due to a delay in the fault clearing time. During a contingency, the IMs slow down due to the decrease of the electromagnetic torque, which causes the highest consumption of current supply and reactive power of the power grid, triggering a higher depression in the service voltage. After clearing the contingency, the electromagnetic torque recovers. If the IM has not decelerated below its critical speed, it accelerates back to a normal operating point. Otherwise, it cannot accelerate again, and it stops (stalls) completely. Stopped IMs can be switched off by under voltage actuation protection schemes or remain switched on resulting in a considerable consumption of start-up type current until they are switched off by a thermal overcurrent protection. In this last case, the voltage remains depressed for a longer time, possibly inducing a widespread cascading collapse in other loads due to the voltage decrease.

In relation to the modeling of the IM, a third order model has been considered, whose equivalent circuit in steady state is shown in Fig. 3 (a). The electrical power demand of the IM is related to the machine parameters, slip, and supply voltage, mathematically calculated according to expression (4). Additionally, the dynamic behavior of the slip S of the IM is calculated according to (5).

$$P_e = \frac{U^2}{\left(\frac{R_r}{S}\right)^2 + (X_r + X_s)^2}\frac{R_r}{S} \tag{4}$$

$$2H_m\frac{dS}{dt} = (T_m - T_e) = \left(\frac{P_m}{1-S} - P_e\right) \tag{5}$$

where H_m is the constant inertia of the machine, P_m is the mechanical load applied to the motor, P_e is the electrical power demanded by the IM disregarding stator losses, and T_e and T_m are the electrical and mechanical torques, respectively. When the mechanical torque T_m is constant, the IM consumes constant electrical power at steady state. Regardless of the applied voltage, the IM operates in the stable region according to the characteristics of the torque-slip curve shown in Fig. 3 (b). The peak torque T_p occurs for slip S_p. The IM operates stably with slip equal to S_1 in the region ($0<S<S_p$), for which the mechanical torque is less than the peak torque. However, during low voltage events or supply voltage disturbances, the IM incurs a slowdown because $T_m>T_e$ and slip continues to increase until the disturbance is cleared, and the voltage level is restored. But, if the slip exceeds S_p in the interval ($S_p<S_2<1$), it implies that the IM enters an unstable region, continues its deceleration and it will eventually cause the motor to stop, if control actions are not taken into account. In this braking condition, the current demanded by the motor is high, causing the voltage to drop uncontrollably. In this situation, the slip S_2 is considered a point of instability [48].

2) AIR CONDITIONING

The A/C systems have fans in the subsystems of condensing and evaporating elements, respectively, and a low inertia induction motor in the compressor system. The two fans consume in regular operating conditions approximately 20% of the total power of the unit, while the compressor (IM) consumes 80% of the remaining power demand [49]. The schematic diagram of A/C components is shown in Fig. 4. The inertia constant of induction motors used in residential A/C systems is very small (usually in the range of 30 ms to 50 ms). This characteristic leads to a rapid deceleration of the A/C IMs during disturbing events in the electrical network that cause the supply voltage to decay. As a result, these motors are highly susceptible to lock-up even in the presence of faults that clear in as few as 3 cycles [5].

To model the dynamic behavior of the A/C system, some techniques reported in the specialized literature shown that several of them focused on the analysis of large power systems. However, the consideration of models that are adapted to residential or microgrid electricity systems have been little reported in the literature. Consequently, this work focuses on the modeling of A/C type loads based on a hybrid model which includes dynamic and static load components, to be able to reproduce the FIDVR phenomenon and the dynamic response of the supply voltage after the occurrence of contingencies that compromise the DVS. The scheme used for

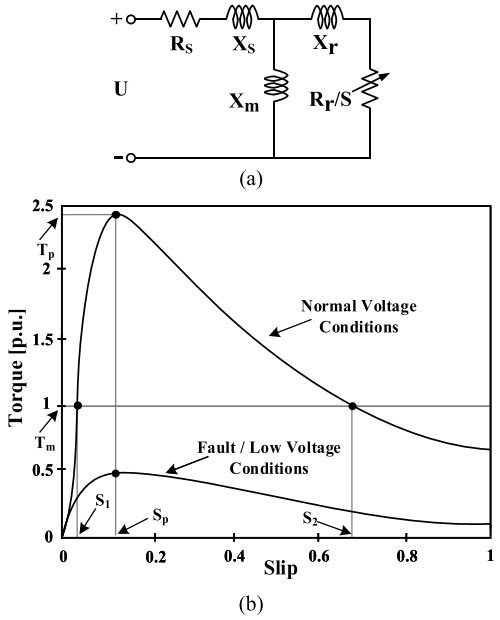

FIGURE 3. (a) Equivalent circuit of the induction motor. (b) Performance curve of the induction motor as a function of toque and slip.

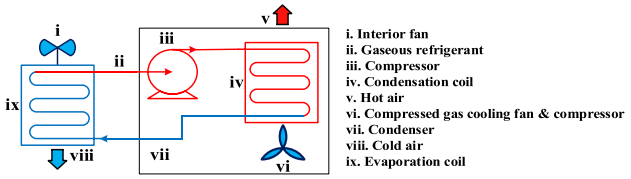

FIGURE 4. Schematic diagram of components for A/C operation.

TABLE 1. Parameters for A/C load modeling static part.

P	aP	0.5	e_aP	2
	bP	0.3	e_bP	1
	cP	0.2	e_cP	2
Q	aQ	0.6	e_aQ	2
	bQ	0.2	e_bQ	1
	cQ	0.2	e_cQ	2

the hybrid load modeling is implemented in PowerFactory DIgSILENT and shown in Fig. 5.

The static part is considered through exponential polynomial modeling for the active (P) and reactive (Q) powers according to (6) and (7), respectively.

$$P = P_0 \cdot \left[aP \left(\frac{V}{V_0}\right)^{e\_aP} + bP \left(\frac{V}{V_0}\right)^{e\_bP} + cP \left(\frac{V}{V_0}\right)^{e\_cP} \right] \tag{6}$$

$$Q = Q_0 \cdot \left[aQ \left(\frac{V}{V_0}\right)^{e\_aQ} + bQ \left(\frac{V}{V_0}\right)^{e\_bQ} + cQ \left(\frac{V}{V_0}\right)^{e\_cQ} \right] \tag{7}$$

where P_0 and Q_0 are the nominal powers of the A/C. aP, bP, cP; aQ, bQ, cQ are the proportional coefficients of the

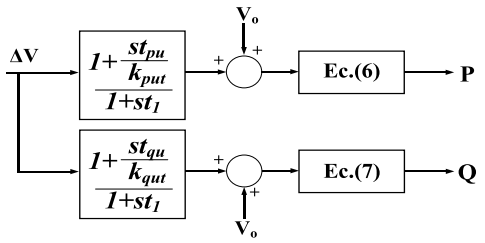

FIGURE 5. Hybrid A/C-type load modeling.

static part of the load, e_aP, e_bP,e_cP;e_aQ, e_bQ, e_cQ are the exponential coefficients of the static part of the load and V is the magnitude of the bus voltage (1 p.u.). V_0 is the absolute voltage, where the A/C is connected (voltage pre-contingence) [50]. Thus, the parameters considered in the modeling are shown in Table 1.

On the other hand, the dynamic component was modeled according to a block diagram scheme depending on the supply and reference voltages of the MG. The corresponding gains for P and Q powers are calculated according to (8) and (9), respectively.

$$k_{put} = aP \cdot k_{pu0} + bP \cdot k_{pu1} + cP \cdot k_{pu} \tag{8}$$

$$k_{qut} = aQ \cdot k_{qu0} + bQ \cdot k_{qu1} + cQ \cdot k_{qu} \tag{9}$$

Those parameters associated with the inertia of the A/C ($T_j = 0.8\ s$) and time constants of the control blocks for the P and Q loops ($t_{pu} = 0.9\ s$; $t_{qu} = 0.9\ s$) were defined according to values reported in [35].

E. FAULT-INDUCED DELAY VOLTAGE RECOVERY

This phenomenon is characterized by the unexpected drop of the voltage modulus in the MG nodes (or buses) after the occurrence of a large disturbance (unscheduled MG isolation or three-phase short circuits, being simultaneous faults of resilient characteristics). Its origin is related to insufficient compensation capacity or reactive power supply. Particularly, this phenomenon is more significant in MGs, because the DERs that make up the MG do not always have dynamic voltage support schemes and control drives that respond quickly and effectively to severe voltage drops at the time of contingencies. Additionally, this phenomenon is closely related to the increase in reactive power demand of dynamic inductive loads such as induction motors, compressed air systems, and air conditioners. In contingency situations, these loads demand a large amount of current from the system to maintain their operating conditions. When an IM stops to recover its operability in a FIDVR event, it can demand between 5 to 8 times its nominal reactive power demand [16]. If the reactive power deficit continues in the MG, the FIDVR could cause the motor and A/C loads to stall or stop operating, thereby increasing the likelihood of a rapid voltage collapse due to DVI [51].

The voltage vs. time curve that describes the behavior, characterization, and stages of a FIDVR phenomenon

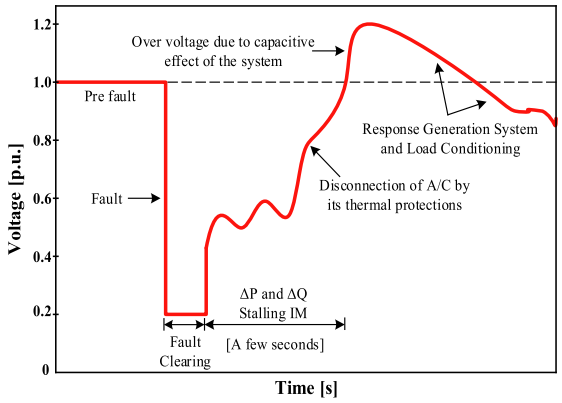

FIGURE 6. Voltage operating characteristics during of a FIDVR event.

is shown in Fig. 6. Firstly, the occurrence of a fault is highlighted. This can be caused by equipment failures or atmospheric conditions; note the depression of the voltage magnitude which produces the A/C braking. Subsequently, the fault is cleared by the protection and switching mechanisms. Consequently, the voltage drops due to the stopping of the A/C system caused by the sudden and rapid variation of the active and reactive power demand which led to recover of the previous voltage in a forced way. Under this condition, the thermal protections of the A/C disconnect it from the grid. Subsequently, overvoltage and later under voltage occur due to the capacitive effect of the connected power system components. Finally, system normalization occurs due to the response of the generation system to load conditioning, which stabilizes the voltage at pre-contingency or under-voltage conditions [52].

The main FIDVR events have been recorded initially in the California electrical system in the USA and over the years this phenomenon has become present in other sites of the world. Mainly, the FIDVR phenomenon has been detected and recorded by the installation of phasor measurement units (PMUs). In the following, the FIDVR events recorded in different locations and their significant consequences, as well as different hypotheses, models, and mitigation alternatives to face FIDVR in contemporary power systems and MGs will be briefly treated. A representative case was observed in Southeastern California in 2014. In the summertime, the massive connection of A/C systems for cooling and ventilation systems, added to the prevailing atmospheric conditions with a large number of lightning, led to the recurrent disconnections of transmission lines. Consequently, there were several problems to control and maintain stable voltage in the sub-transmission and distribution buses, which originate considerable appearances of FIDVR [52]. In this sense, in order to study in-depth, the characterization of this FIDVR phenomenon and to establish corrective actions in case of a new and eventual occurrence, researchers proposed in [5] a methodology that allowed modeling load components based on measurements and characterization that directly influences the occurrence of FIDVR. On the other hand, at the Entergy Texas power system a logical load-shedding strategy based on multifunctional relays was proposed [53] to prevent FIDVR from leading to voltage instability and collapse. In addition, researchers present in [54] a machine learning approach based on real-time measurements and data that allows establishing an adaptive voltage control method to mitigate FIDVR in a fast response time to avoid instabilities. Another important approach to correlating the FIDVR between a failure in the power system and the ambient temperature is the work presented in [55], where through multiple simulations, it manages to obtain the worst operating condition that resolved in a real FIDVR phenomenon in the Iranian system. This occurs in the hottest hours and therefore with greater demand for residential A/C use. The model reproduced by simulations, mimicked the real records. On the other hand, specifically related to MGs, the work proposed in [56] exposes an adaptive load-shedding scheme to mitigate FIDVR through dispersed synchronous generators. The innovative aspect of this methodology is the use of the gradient of the imaginary part of the admittance to discriminate FIDVR events that produce instabilities and those that do not through load-shedding. Another approach is presented in [57], where using PMUs in distribution systems, it is estimated the voltage recovery time before a FIDVR event. Additionally, using linear optimization it is possible to control the A/C type loads for optimal reactive power injection of DERs to mitigate FIDVR. Therefore, over the years it has been shown that research due to FIDVR characterization and its tightness with voltage control has fundamental correlations, whereas, at the microgrid level few contributions have been explored to characterize FIDVR and DVS. The actions and mechanisms to mitigate and/or avoid FIDVR in MGs correspond to fast controls in DERs, mainly with LVRT characteristics, incorporation of FACTS reactive power compensation devices (SVC, DSTATCOM), fast protection schemes and fault clearing, mainly avoiding load disconnections, which reduces operational resilience and can even intensify the presence of FIDVR.

III. RESILIENCE ASSESSMENT METRIC BASED ON A PROBABILISTIC POISSON MODEL

Presently, the analysis of disruptive events derived from non-frequently occurring contingencies has gained prominence in the world's power systems. These events of low probability of occurrence which cause serious and important operational, or infrastructure impacts are called resilient events. Due to their topological and infrastructure characteristics, MGs are more susceptible to being affected by this type of contingencies, decreasing the level of their resilience, and compromising their stability. In this sense, maintaining dynamic voltage stability is quite difficult due to the occurrence of resilient contingencies that trigger the operational isolation of the MG. Therefore, there is a need to quantitatively evaluate the level of resilience of a microgrid under these operating conditions.

Based on the above, a mathematical model based on the Poisson probability distribution is proposed, to evaluate the simultaneous contingencies that could occur in the MG based on the statistical information of contingencies that have occurred. For this purpose and taking as a methodological input what is presented in [58], historical data related to faults due only to short circuits in the electrical system of the United Kingdom (Wales-England) are shown, where the annual occurrence of almost 300 contingencies was recorded. From these contingencies, 3% were double ground faults, 5% were three-phase ground faults, 25% were two-phase faults between phases and the remaining 67% corresponded to single-phase faults [59]. From this, it is clear that those contingencies of double ground faults and three-phase to-ground are the ones with the lowest frequency of occurrence. Thus, in this quantitative analysis of resilience, the focus will be placed on three-phase ground faults, and it will be assumed the percentage of double ground faults as input for the other simultaneous three-phase contingency, taking as hypothetical resources the aforementioned historical records. To quantify probabilistically this situation, the simultaneous double contingency of type (N-1-1), the first one due to the operational isolation of the MG and the second one due to the disconnection caused by a failure in an MG feeder are taken into account; all this in concomitance with the definition of the resilience of electrical systems and particularly in MGs [12]. The premise considered is that the occurrence of one of the contingencies causes the isolation of the MG and the following contingency further compromises the stability of the microgrid analyzed from the perspective of the dynamic performance of the voltage. To achieve this objective, the probabilistic mathematical criterion performs a Poisson model, whose expression is shown in (10). The adoption of this model is noteworthy because, with this probability distribution it is possible to analyze and correlate in a combinatorial way, discrete events associated with independent random variables such as contingencies due to short circuits.

$$\begin{aligned} A \sim Poi\left(\lambda_1\right) \ and \ B \sim Poi(\lambda_2) \\ \{A+B=n\} \rightarrow \{A=k, B=n-k\}; 0 \leq k \leq n \\ Poi\left(A+B=n\right) = \sum_{k=0}^{n} Poi\left(A=k, B=n-k\right) \\ = \frac{e^{-(\lambda_1+\lambda_2)} \cdot \left(\lambda_1+\lambda_2\right)^n}{n!} = \mathbb{R}, \end{aligned} \tag{10}$$

where $\mathbb{R}$ represents the probability of success for the double simultaneous contingencies. Variables A and B represent the contingencies N-1 of isolation and N-1 of disconnection of the MG feeder, respectively. λ_1 and λ_2 correspond respectively to the historical failure percent and, n is the success number to resilient events that is desired to analyze. For this study, all annual joint faults have an occurrence of 24 events. to show the characteristic of resilient events, a $k = 30$ was considered in both cases. The probability distributions for each of these contingencies are shown in Fig. 7.

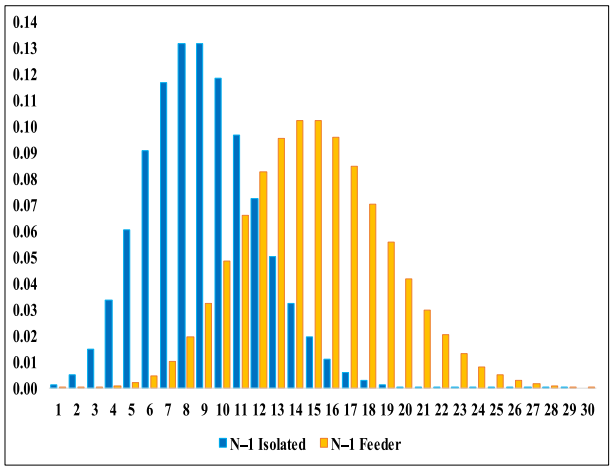

FIGURE 7. Poisson distribution under resilient contingence.

TABLE 2. Probabilistic model simultaneous contingencies N–1–1.

Multi-scenario resilient disruptive events probability $\mathbb{R}$								
	Sce $\mathbb{R}$ 1	Sce $\mathbb{R}$ 2	Sce $\mathbb{R}$ 3	Sce $\mathbb{R}$ 4	Sce $\mathbb{R}$ 5	Sce $\mathbb{R}$ 6	Sce $\mathbb{R}$ 7	Sce $\mathbb{R}$ 8
n=2	λ_1=1 λ_2=1	λ_1=2 λ_2=1	λ_1=3 λ_2=1	λ_1=4 λ_2=1	λ_1=5 λ_2=1	λ_1=6 λ_2=1	λ_1=7 λ_2=1	λ_1=8 λ_2=1
$\mathbb{R}$	0.271	0.224	0.147	0.084	0.045	0.022	0.011	0.005

Accordingly, (10) has been used to quantify the simultaneous double contingency incurred by the MG. This quantitative evaluation considers the different failure rates associated with each disturbance based on their historical averages and for different scenarios. Thus, the variation of λ_1 and λ_2 (the hypothetical consideration is that the feeder that connects the MG with the larger grid has a higher failure rate than the internal feeder of the MG). So, the success probabilities for the double contingency scenario N-1-1 are summarized in Table 2. Although the Poisson distribution is used for probabilistic events of discrete independent variables, to better show the probabilistic distribution for the N-1-1 simultaneous double contingency event, the probability functions are presented continuously in Fig. 8.

To quantify and correlate both, the probabilistic resilience approach $\mathbb{R}$ and the DVS analysis (based on the performance indices shown in section II), an expression based on the mathematical expectation $\mathbb{E}$ for each resilient contingency scenario *Sce i* is presented in (11).

$$\mathbb{E}\left[A+B\right]_{Sce\ i} = \mathbb{R} \cdot \sum_{Sce\ i} \left(VDI_j^k + TDVSI_j^k - DVPI_j^k\right) \tag{11}$$

IV. FACTS DEVICES AND SMART INVERTERS

Devices based on FACTS controllers have been widely used in large power systems. Specifically, the SVC and DSTATCOM are the devices that have given the best results for voltage stability due to their fast reactive power injection despite their dissimilar functional characteristics. Due to their

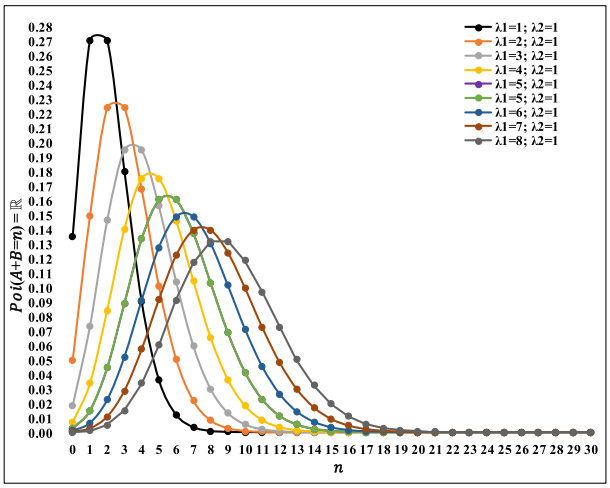

FIGURE 8. Poisson ℝ probability distributions: resilient events.

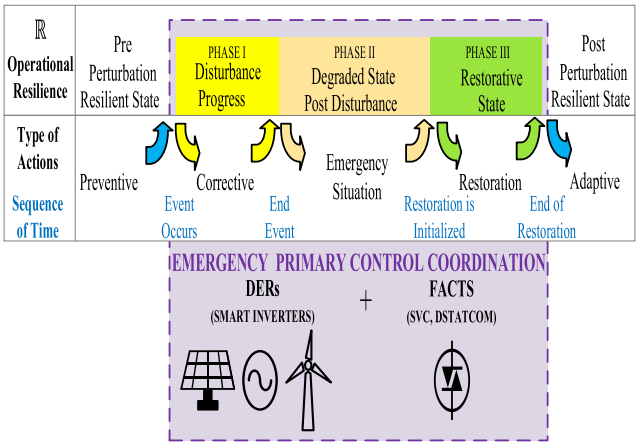

FIGURE 9. Relationship between FACTS, smart inverters and operational resilience.

shunt connection characteristics, they allow for improving the dynamic control of reactive power and consequently of voltage [60]. The inner characteristics of FACTS devices based on power electronics equipment, allow them to provide fast controls and operational versatility aiming at improving the dynamic behavior of the electrical system. However, with the recent rise of microgrids, due to their topology characteristics and modes of operation, technical difficulties have arisen that compromise their operation and stability. Indeed, they have demonstrated difficulties in maintaining stable voltage when the microgrid incurs its unscheduled operational isolation due to the occurrence of contingencies. In this sense, new problems related to voltage stability have appeared, which have been little addressed in the specialized literature, among which stand out the isolation operation of MGs. In these conditions, MGs are forced to operate autonomously and independently to preserve their stability conditions and provide continuity in the electric power supply within adequate operating parameters. This situation of uncontrollability of reactive power is worsened when the MG is affected by contingencies of resilient characteristics. In these cases, the EPCs associated with solar and wind DERs of the MG must have LVRT characteristics and dynamic reactive power control, to maintain voltage stability and avoid system collapse. Therefore, the models developed for the FACTS devices i.e., SVC and DSTATCOM, and the smart inverter based on the IEEE-1547-2018 standard are developed in the following. All these FACTS devices and inverters operated in a coordinated manner and with a priority strategy to the emergent primary control in case of contingencies can contribute to improving the operational resilience in the MG, as shown in Fig. 9 [60].

In this context, the research developed in this work is intended to demonstrate the applicability of incorporating FACTS devices connected in shunt mode that, due to their operating response characteristics, can help to solve the problems of dynamic voltage instabilities and guarantee the autonomous operation of isolated MGs. Additionally, it is

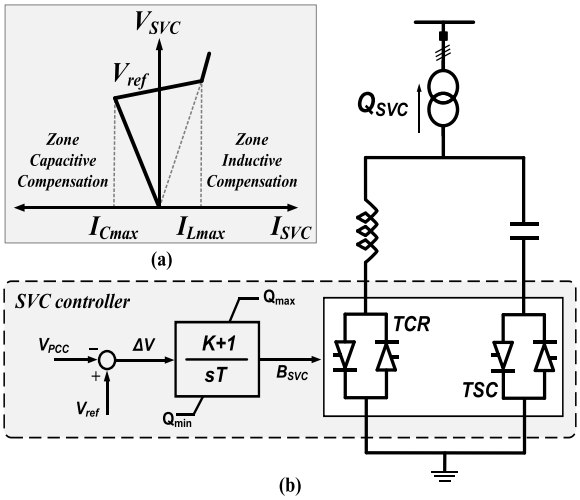

FIGURE 10. (a) Operating diagram of an SVC. (b) Control diagram and coupling diagram of the SVC to the MG.

intended to establish a comparative relationship based on the performance and dynamic response between the SVC and the DSTATCOM to demonstrate which of these FACTS devices can achieve superior results to improve the dynamic voltage stability of MGs subject to extreme operating conditions such as resilient contingencies. Finally, the proposal of this work aims to contribute to considering the FACTS device technology as an operative mechanism that allows contributing to the analysis and solution of the detriment of the operational resilience that in microgrids is closely related to the stability analysis. In addition, the analysis of operational resilience should be included as a fundamental part of the study of stability in its multiple aspects in electrical systems, particularly in microgrids. Based on the proposal of this work and the results obtained, it is expected that a new research area can be envisioned that incorporates other types of FACTS devices to solve other stability problems in MGs and consequently improve their resilience.

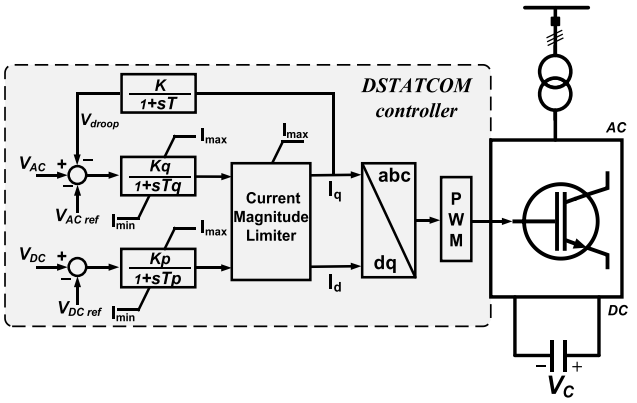

FIGURE 11. Operating diagram of a DSTATCOM coupling to the MG and its respective controller.

A. STATIC VAR COMPENSATOR (SVC)

Historically, the SVC device was one of the first developments of FACTS technology in bulk power systems. Its operational performance is related to its fast reactive power compensation and controllability. The operation of the SVC in terms of its injection current to keep the voltage in the (V_{SVC}) connection zone under control is shown in Fig. 10 (a). For this purpose, a certain control slope is assumed, which represents the variation of the injection current in response to deviations from the reference voltage (V_{ref}). The operation of the SVC is limited by the thyristors that compose it and according to their maximum current contributions from either the inductive or capacitive zone. An SVC device operates in the capacitive zone if $B_{SVC} > 0$ and in the inductive zone if $B_{SVC} < 0$. If the limits of control currents in the SVC are exceeded, this device behaves as a pure reactor or constant fixed power capacitor. An SVC is constituted of thyristor-controlled reactors (TCR) and thyristor-switched capacitors (TSC). The combined switching of the TCRs and TSCs allow continuous control of either absorption or reactive power supply through the SVC current, which allows it to maintain an adequate voltage profile at the connection node in the steady and dynamic states [61]. In Fig. 10 (b), an SVC is shown schematically with its components; its coupling to the MG system is through a transformer and its respective control diagram. The control scheme consists of measuring and comparing the voltage signals of the connection node with the reference voltage. Then this signal is coupled to a PI controller that is limited in terms of the rated reactive power of the SVC. The output of the control signal will allow, through its susceptance, to perform inductive or capacitive reactive power compensation, as appropriate.

B. DISTRIBUTION STATIC COMPENSATOR (DSTATCOM)

The DSTATCOM device emerged later than the SVC. The DSTATCOM is a FACTS technology device whose connection to the MG is shunt. Constitutively, it consists of a voltage source converter fed by a capacitor on the DC side. The converter is in charge of supplying/absorbing reactive power through its control system, which is in charge of sensing the current and voltage from the AC side. Generally, the converter uses semiconductor elements with turn-off capabilities, such as GTO (Gate Turn-Off) thyristors or IGBT (Insulated Gate Bipolar Transistors) devices. The highlight of the DSTATCOM is that it can provide dynamic voltage support of either inductive or capacitive characteristics without needing reactor banks or capacitors [61], [62]. An important advantage of this device is that its capacity is limited only by the nominal capacity of the converter, and it does not depend on the voltage profile of the MG. The DSTATCOM modeled for this study is shown in Fig. 11, which considers a VSC with PWM (pulse-width modulation) using IGBTs.

C. SMART INVERTERS BASED ON STD IEEE-1547-2018

Formerly, inverters associated with renewable generation sources had as an operational premise when disturbances occurred to disconnect due to their overcurrent protection scheme. However, with the recent publications of the IEEE-1547-2018 standard and updated grid codes, new premises and operational requirements are put forward for the behavior and dynamic performance of these inverters. That is, in case of contingencies these inverters must not disconnect from the grid. Instead, they must have responsiveness in dynamic support mode for voltage and reactive power. This is not so with the active power that, to protect the inverter from excessive over-currents during the contingency time, its active power must be reduced to zero until the disturbance is cleared. Thus, the premise is the recovery of the pre-fault active power supply once the disturbance is cleared. This measure ensures the safety and reliability of the system. Inverters that meet these operational requirements are known as ''smart''.

The control criteria and assumptions used to model the inverters used in the case studies that will be presented later are shown below. Regulation-based requirements have been shown to require the operation of dynamic voltage support schemes for inverters associated with DERs under contingency conditions.

In this section, the modeling carried out on a smart inverter is presented to comply with the LVRT scheme. The simplified LVRT control scheme based on IEEE Std 1547-2018 of the three-phase smart inverter is shown in Fig. 12, which is used in the study for both MG DERs, that is the solar PV and the grid-side inverter of the wind farm. The block named LVRT Control has been parameterized according to the characteristics shown in Fig. 2 so that the inverter operation is considered as smart. Reactive and active power blocks allow coordinated operation in the IV quadrants of the inverter. In the modeling, the scheme has been prioritized in dynamic voltage support operating mode for resilient fault conditions. The reactive power control block is the one that is constantly controlling the voltage at the inverter terminals, to detect variations in its magnitude and coordinate with the LVRT control block. In this LVRT control block, the dynamic voltage control scheme is established. In this case, the control premises are

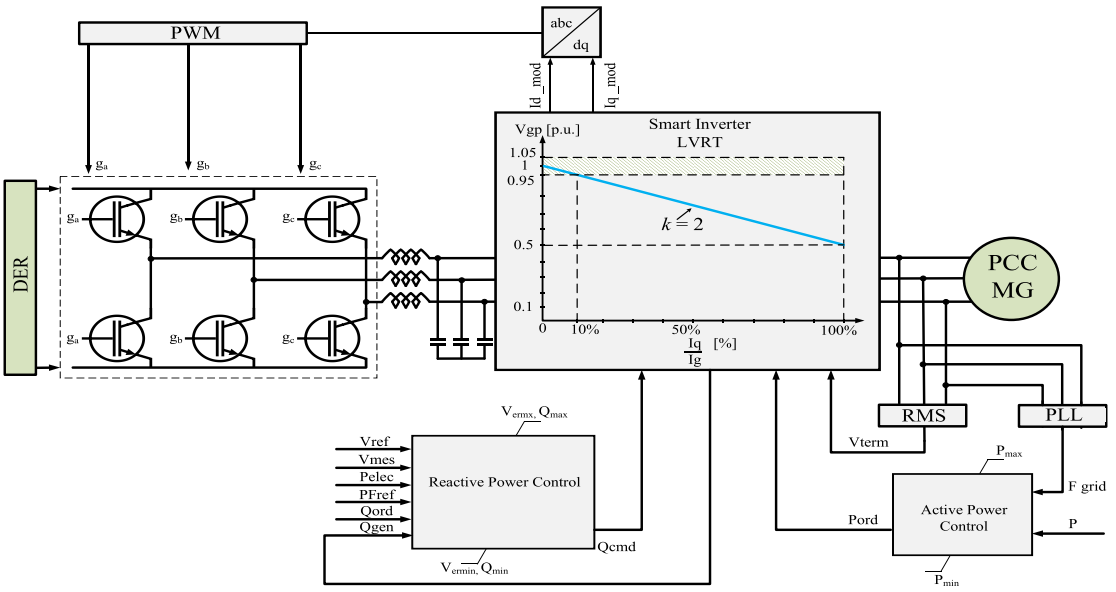

FIGURE 12. Modeling of smart inverter to DERs and control LVRT based on IEEE Std 1547-2018.

that the inverter associated with the DER remains connected with voltages above 0.50 p.u. In these conditions, the DER must inject a capacitive reactive current (+Q), for which, voltages and currents in the inverter are related as follows: the voltage V_n corresponds to the nominal positive sequence voltage at the point of common coupling or PCC, ΔI_q, is the relative amount of capacitive (+Q) or inductive (–Q) current injected by the DER under disturbing conditions and ΔV_f is the relative change in the PCC voltage during the fault. Mathematically, ΔI_q and ΔV_f are related according to (12) and (13), respectively:

$$\Delta I_q = I_q - I_{q0} \tag{12}$$

$$\Delta V_f = V_f - V_n, \tag{13}$$

where I_q is the DER reactive current that is injected during the disturbance, I_{q0} is the pre-disturbance output reactive current of the same DER, and V_f is the direct sequence voltage of the PCC during the disturbance. Additionally, the smart inverter of the DER must respond dynamically and mandatorily to the minimum LVRT time with a time vs. voltage slope equal to 4 s/1 p.u. when the voltage falls between 0.70 p.u. and 0.88 p.u. [47]. Besides, the active power control block monitors the system frequency and coordinates the operation of the power supply under normal operating conditions, while under disturbances it acts in coordination with the reactive power and LVRT blocks. In the section corresponding to the case study, the compliance and operational response of smart inverters for the two DER technologies considered in the microgrid will be shown through computer simulations. To establish a control strategy and dynamic voltage support, it is initiated from the consideration of reactive current and its injection based on the sudden voltage drop at the time of

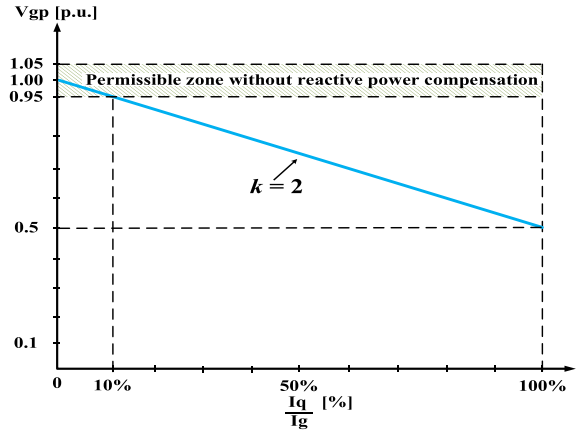

FIGURE 13. Reactive current as a function of voltage for smart inverter modeling.

contingencies. The operational criteria for the control strategy are adopted from [8] and modified to reproduce the smart behavior of the inverters associated with DERs in MGs systems. Therefore, the inverter injection reactive current I_q is defined as follows in (14) and its behavior is determined by Fig. 13:

$$I_q = k(1 - V_{gp}) \cdot I_g \tag{14}$$

where I_g is the magnitude of the grid current, V_{gp} is the operation voltage and k is a proportional scaling factor defined by (15).

$$k = \frac{(I_q - I_{qo})}{I_g \cdot (1 - V_{gp})} \tag{15}$$

TABLE 3. Multi-scenario steady-state DERs generation dispatch.

	Demand scenario 1 IM 60%; ZIP-PQ 40%		Demand scenario 2 IM 30%; ZIP-PQ 70%	
DERs	kW	kVAr	kW	kVAr
Solar Photovoltaic	4000	0	4000	0
Wind Generation	1500	0	1500	0
Synchronous Machine	2627	5000	2576	5000
Link grid-MG	25	14	25	14

TABLE 4. Steady-state demand scenarios.

	Demand scenario 1 IM 60%; ZIP-PQ 40%		Demand scenario 2 IM 30%; ZIP-PQ 70%	
Type of load	kW	kVAr	kW	kVAr
Dynamic loads	3481.6	2611.3	1776.9	1305.7
Static loads	4650.5	2427.1	6329.9	3686.4

where I_{qo} is the initial value of the reactive current under pre-fault conditions. When considering the premise that the voltage operates in the permissible band of ±0.05 p.u. wconcerningthe nominal voltage (1 p.u.), this implies that $I_{qo} = 0$. International grid codes establish that $k \geq 2$, thus guaranteeing 100% injection of the reactive current in the transient state, in accordance with the voltage threshold premise of 0.50 p.u.

Under normal operating conditions, the control strategy is the maximization of active power injection from DERs. On the contrary, the strategy used for injection current is prioritized with respect to reactive power only in contingency situations. Thus, the maximum injection current $I_{gmáx}$ of the inverter is calculated according to (16).

$$I_{gmáx} = m \cdot I_m = constant \tag{16}$$

where I_m is the rated current of the smart inverter, m is the scaling factor of the peak current reached for power derating operations. When the instantaneous voltage of the DER connection node decreases due to resilient disturbances, two conditions are presented for the control strategy.

i) if the voltage decreases at the rate of the range $[(1 - 1/k) \leq V_{gp} \leq 0.95]$, the injection current to the grid defined in the reference frame *qd*, is defined according to (17) and (18), respectively.

$$I_q = k(1 - V_{gp})/I_m \tag{17}$$

$$I_d = \sqrt{m^2 - k^2(1 - V_{gp}^2)I_m} \tag{18}$$

ii) this condition considers a sudden drop when the instantaneous voltage is limited according to $[V_{gp} \leq (1 - 1/k)]$, the injection current in the reference frame *qd* is determined by (19) and (20), respectively.

$$I_q = I_m \tag{19}$$

$$I_d = \sqrt{m^2 - 1} \cdot I_m \tag{20}$$

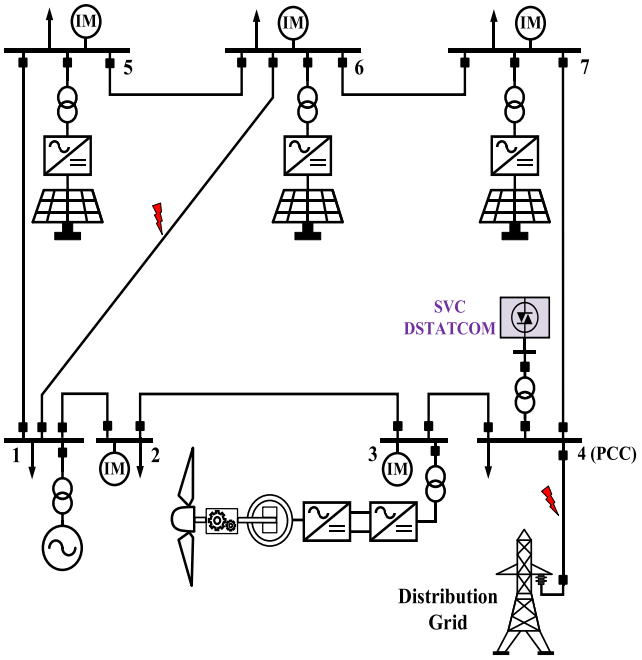

FIGURE 14. Single-line diagram of microgrid test system [40].

TABLE 5. Load participation in different operating scenarios.

Operating Scenario	IM [%]	PQ [%]	Fault location [%]
1	60	40	63.5
2	60	40	36.5
3	30	70	63.5
4	30	70	36.5

V. CASE STUDIES AND TEST SYSTEMS

A. TEST SYSTEM 1–MICROGRID

For the analysis of the first study case, the test MG reported in [40] is taken into account, in which modifications were made in terms of the power generated and dispatched mostly from non-conventional renewable energy sources and the inclusion of dynamic loads. The single-line diagram of the MG is shown in Fig. 14. In this MG, the participation of 3 different DER technologies is highlighted: solar photovoltaic, wind power (type IV) using a full converter, and conventional generation based on the synchronous machine. The steady-state generation dispatches of each of the DER technologies are shown in Table 3, as well as the exchange of power flows from the equivalent distribution grid to which the microgrid is interconnected. In addition, the demand component is made up of dynamic loads such as induction motors and static loads modeled from impedances and constant powers (ZIP and P-Q). Different percentage shares of the static and dynamic load components have been considered according to the study case scenarios and are shown in Table 4. Finally, the 4 operational scenarios considered for the analysis are included in Table 5. For these scenarios, the occurrence of contingencies originated by three-phase faults

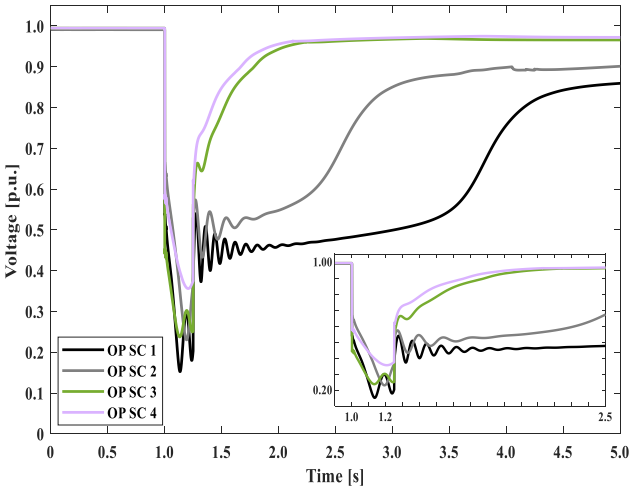

FIGURE 15. Dynamic voltage performance under different resilient contingencies and different operating scenarios without FACTS.

(short circuits) located at 36.5% and 63.5% of the length of the medium voltage line that interconnects the MG and distribution grid were considered. For this reason, and to analyze resilient contingency scenarios, an additional simultaneous contingency has been considered in one of the MG feeders. This is a three-phase fault at 50% of the feeder length. In other words, there are 8 possible simultaneous resilient contingencies of type N-1-1 that can occur in the MG-grid system. The simulation process has an analysis time frame of 5 s according to the short time DVS analysis criteria. The simultaneous contingencies considered occur at 1 s from the beginning of the simulation process. For both resilient contingencies, a fault detection and clearing time equal to 0.25 s has been considered. Therefore, to quantitatively evaluate the DVS of the MG, the three performance indexes presented in section II have been taken as methodological input to determine the N-1-1 simultaneous resilient contingency, which compromises in a worse way the dynamic voltage stability of the whole MG. Thus, the results of the sensitivity analysis with their respective simulations corresponding to all the resilient contingencies and whose quantitative evaluation is based on the three voltage performance indexes are presented in Table 6. Therefore, due to the low variability in the indexes between resilient contingencies 1 and 3, it was determined by consensus that the simultaneous contingency listed as 4 (Grid-PCC line and MG feeder 1-6) is the one that will be taken into account and will serve as the basis for the analysis of the next study cases that include the incorporation of SVC and DSTATCOM FACTS devices to improve the dynamic voltage stability. The PCC node is also called node number 4.

Additionally, the dynamic voltage performance for the analyzed contingencies is shown in Fig. 15. As demonstrated in the analyzed operational and resilient contingency scenarios, all of them have an outcome of dynamic voltage instability, late voltage recovery, low voltage profile, and the presence

TABLE 6. Dynamic voltage performance indices from the sensitivity analysis to different n-1-1 simultaneous resilient contingencies and operating scenarios.

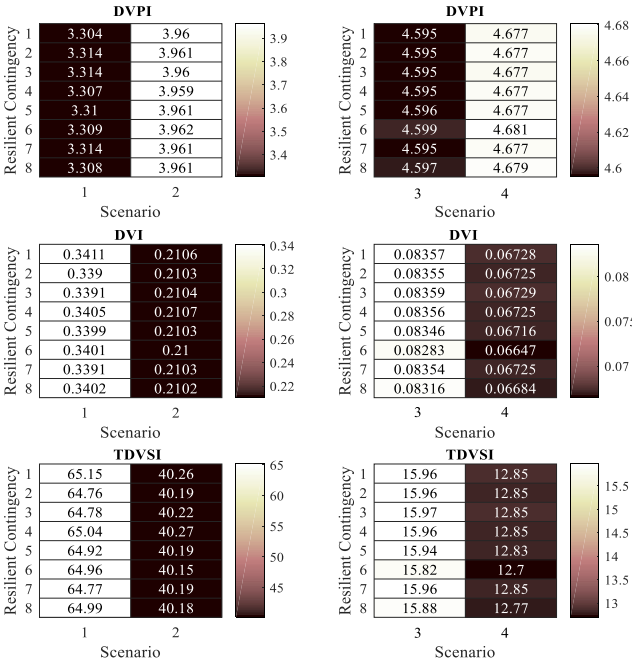

TABLE 7. Optimal location of FACTS: SVC and DSTATCOM devices in the microgrid to improve DVS.

Operational Scenario	SVC		DSTATCOM	
	Node Location	Optimal Value	Node Location	Optimal Value
1	1	18.24678	PCC	11.96272
2	1	9.27495	PCC	6.30809
3	PCC	4.51716	PCC	4.16053
4	PCC	2.25236	PCC	1.95738

of the FIDVR phenomenon. For operating scenario 1, a voltage collapse is shown, due to the presence of most of the dynamic load in the MG and the proximity in the location of the short circuit to the PCC node. Given the above, it is justified the need and adoption of FACTS devices, whose dynamic reactive power compensation allows for mitigating these operational drawbacks and phenomena related to the voltage performance of the isolated MG. Therefore, to analyze and evaluate the improvements in the dynamic voltage stability with the incorporation of SVC and DSTATCOM devices, the following section proposes a methodology that allows to optimally locate the connection of such FACTS in the MG.

B. OPTIMAL LOCATION OF FACTS IN THE MICROGRID

The methodology developed for the optimal location of FACTS devices to improve the DVS is presented in this section, considering the occurrence of resilient contingencies that cause the operational isolation of the MG. To this aim, it is assumed that any of the two types of FACTS devices

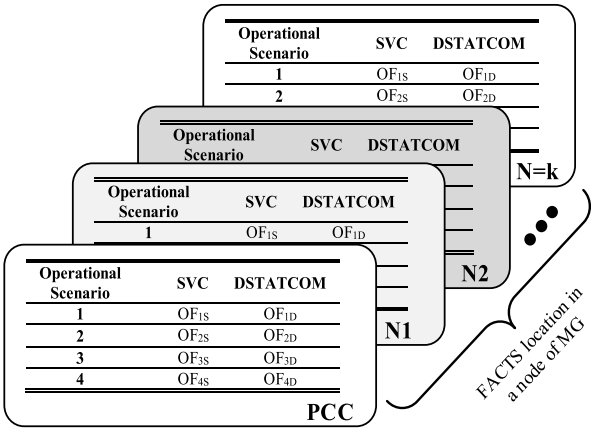

FIGURE 16. Evaluation of the objective function for optimal FACTS location in multiple operational scenarios of the MG.

can be connected to a single node of the MG, but not both devices at the same time because a comparative analysis of the operational performance between the SVC and DSTATCOM will be performed. Next, the computational modeling of these FACTS devices was performed in the PowerFactory DIgSILENT software, these models are consistent with those presented in section IV. Considering two different FACTS technologies, which can cause variations in the operating performance of the voltage in the MG to the occurrence of the same contingency, the objective of this research is to analyze comparatively which of them gives improvements to the DVS. To carry out this stage of analysis, a script was developed in PowerFactory DIgSILENT software, to simulate all contingencies and operating scenarios in which the MG incurs in its operation. The total number of analyzed cases corresponds to 56 (4 operational scenarios × 7 candidate connection nodes × 2 FACTS devices). With the results obtained from these simulations, we proceed to discretize the voltage vs. time signals aiming at calculating the dynamic voltage stability performance indices in the Python environment for each case of study. For this, a mixed integer linear optimization model is proposed, whose formulation is based on the calculated voltage performance indices, to avoid nonlinearities in the optimization problem. Therefore, the objective function is expressed according to (21). Regarding the constraints, the condition that allows the connection/disconnection of the FACTS device in each of the MG nodes is shown in (22). In turn, to ensure that there is no reactive power overcompensation due to the connection of the FACTS in the MG, it is considered that the maximum rated reactive power for the SVC and the DSTATCOM should not exceed the maximum reactive power demand of loads (static and dynamic) involved in the MG as expressed in (23). Complementarily, other restrictions are shown in (24), (25), and (26) that consist in setting minimum and maximum thresholds, as appropriate, for each of the voltage performance indices. The restrictions of the indexes were established as inequality conditions that allow guaranteeing the permissible voltage operating limits, as well as to reduce the computational processing times of scenarios that would not improve the dynamic voltage stability of the microgrid. The determination of the index limits for each of the constraints has been performed separately, so that each of them reflects the operational condition of voltage stability due to compliance with the operational limits of the network code, which was performed at a stage previous to the global analysis shown. Finally, in the global objective function it is possible to obtain the nodal location of each FACTS device considered that allowed to achieve the best conditions of dynamic voltage stability in the microgrid. These, with the dynamic reactive power contributions of the FACTS devices in coordination with the LVRT operation of the smart inverters associated with the DERs, guarantee improvements in the dynamic stability of the voltage in the isolated MG, after resilient disturbances.

$$OF: min \sum_{k}^{N} U_z \cdot \left[VDI_j^k + TDVSI_j^k - DVPI_j^k \right] \tag{21}$$

$$\forall k \epsilon \{PCC, 1, \ldots, N = 7\}$$

$$s.t.: \quad \sum_{k}^{N} U_z = 1; \tag{22}$$

$$U_z = \begin{cases} 1 & \text{if FACTS is in node k} \\ 0 & \text{if without FACTS is in node k} \end{cases}$$

$$0 \leq Q_{FACTS} \leq (Q_{ZIP+PQ}) + Q_{IM} \tag{23}$$

$$4.62108 \leq DVPI_j^k \leq 5.0 \tag{24}$$

$$12 \leq TDVSI_j^k \leq 15 \tag{25}$$

$$0 \leq VDI_j^k \leq 0.03 \tag{26}$$

Once the operational conditions for the simulation stage, its voltage-time signal processing and the PowerFactory-Python (Pyomo) interface [63] have been established. It was proceeded to the mathematical formulation stage with the further development of the optimization algorithm, to determine the optimal location of the FACTS devices in the MG. The analysis scheme used is shown in Fig. 16 as well as the evaluation for each objective function, considering the nodal location of the SVC and DSTATCOM in each of the scenarios that incur operationally in the MG.

The results obtained from the proposed simulation and optimization processes yielded the following results shown in Table 7. It is necessary to highlight that the optimal nodal location for the two FACTS devices used is based according to the operational scenario of the MG. Thus, the minimization of the objective functions achieved showed that in comparative terms, the dynamic operating performance of the DSTATCOM device is superior to the SVC. On the other hand, it has been obtained that for scenarios 1 and 2 linked to the use of the SVC device in the microgrid, its optimal location corresponds to node 1. This situation draw attention because, in the other operational scenarios analyzed for both the SVC and the DSTATCOM, the optimal location of these devices derived in their connection in the PCC of

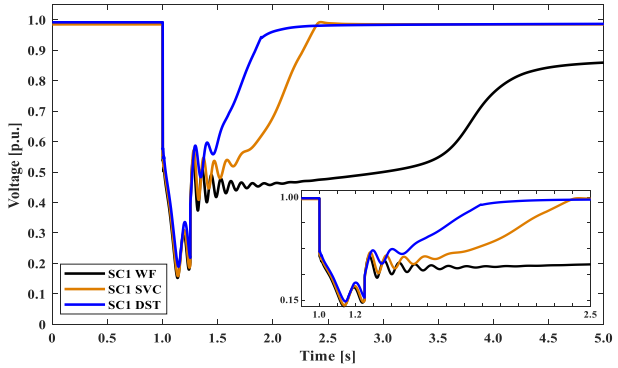

(a)

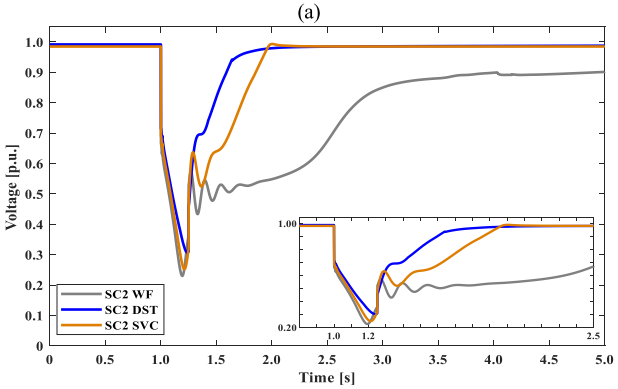

(b)

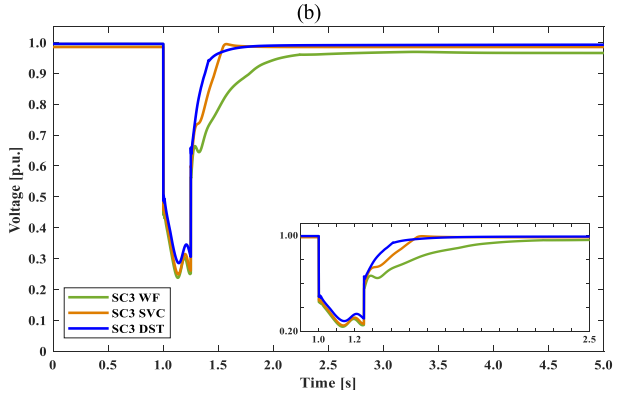

(c)

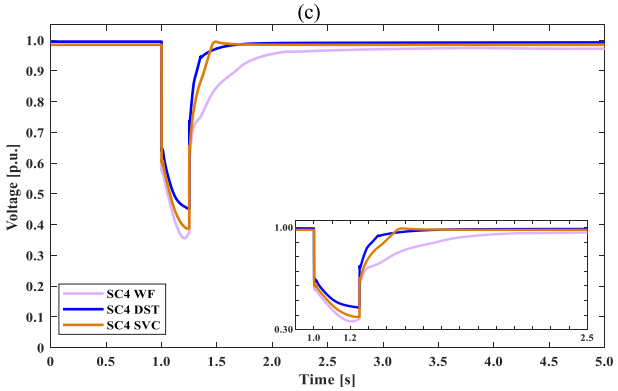

(d)

*(SC: # of scenarios analyzed; WF: without FACTS; SVC; DST: DSTATCOM).

FIGURE 17. Dynamic voltage behavior in the MG without and with FACTS for multiple operating scenarios.

the MG. Based on this, the objective function of the SVC with connection in the PCC node was evaluated for operation scenarios 1 and 2, whose results were 18.28197 and 9.28494, respectively. That is, the percentage variability is 0.19% and 0.11%, respectively, taking as reference the SVC connection at node 1. Therefore, it can be concluded that the best nodal location of both FACTS devices in the MG correspond to the connection at the PCC node. This is so because at this node the dynamic reactive power contributions of the SVC and DSTATCOM will allow an improvement in the performance and dynamic voltage stability in the MG in all demand scenarios and resilient contingencies analyzed.

Subsequently, Fig. 17 shows the dynamic voltage signals for each of the four operating scenarios and for each FACTS device. It is necessary to mention that only the voltages of the MG PCC node are illustrated to comparatively visualize the dynamic performances between the SVC and DSTATCOM (DST) devices and without the presence of FACTS (WF) in the microgrid. It is noticeable that the improvements achieved in the dynamic voltage of the MG are due to the performance of the DSTATCOM for the 4 operating scenarios (SC).

Regarding operating scenario 2 shown in Fig. 17 (b), although the location of the short circuit differs concerning scenario 1, this contingency is more distant from the PCC. But it has not differed its load components in the MG. Therefore, it is shown that there is also a dynamic voltage instability with four oscillations in its signal and a faster presence in temporal terms of the FIDVR phenomenon. The sustained post-disturbance operating voltage reaches a value of 0.88 p.u., which leads to an inoperative scenario even in emergency conditions of the MG for not complying with the grid codes. With the connection of the SVC, there is only an oscillation in the voltage signal and a rapid recovery of the voltage to a value of 0.99 p.u. at 0.75 s after the occurrence of the contingencies (2 s from the beginning of the simulation). On the other hand, with the DSTATCOM device, it is shown that no signal oscillations occur, and the voltage recovery is much faster reaching 0.99 p.u. at 0.50 s after the occurrence of disturbances and at 0.75 s the value of 1.0 p.u. is reached. Another important aspect to highlight is the voltage suppression level at the time of the disturbances, reaching a minimum value of 0.20 p.u. without FACTS. In that sense, with the incorporation of the SVC and DSTATCOM the suppression in the minimum value reached for the voltage corresponded to 0.25 p.u. and 0.32 p.u., respectively.

The results shown in Fig. 17 (c) correspond to operating scenario 3, whose simulations show that with the occurrence of the contingency at 63.5% of the length of the Grid-MG line and with a participation of 30% of dynamic load, the FIDVR phenomenon does not occur without the participation of FACTS in the MG. That is, the voltage signal tends to take a somewhat slow recovery until it reaches a stable voltage level but with a value equal to 0.93 p.u. which violates the lower limit of operability for isolated MG (0.95 p.u.). The minimum voltage drop at the time of contingencies reaches 0.21 p.u. with respect to its nominal value. With the incorporation of the SVC, the minimum voltage is 0.22 p.u., there are no post-disturbance oscillations, and the voltage reaches a

TABLE 8. Superiority in operating performance of DSTATCOM vs. SVC.

Operational Scenario	VDI	TDVSI	DVPI	Objective Function
1	27.13%	27.13%	3.64%	34.57%
2	20.82%	20.82%	1.63%	32.06%
3	3.75%	3.75%	0.18%	7.90%
4	4.07%	4.07%	0.15%	13.10%

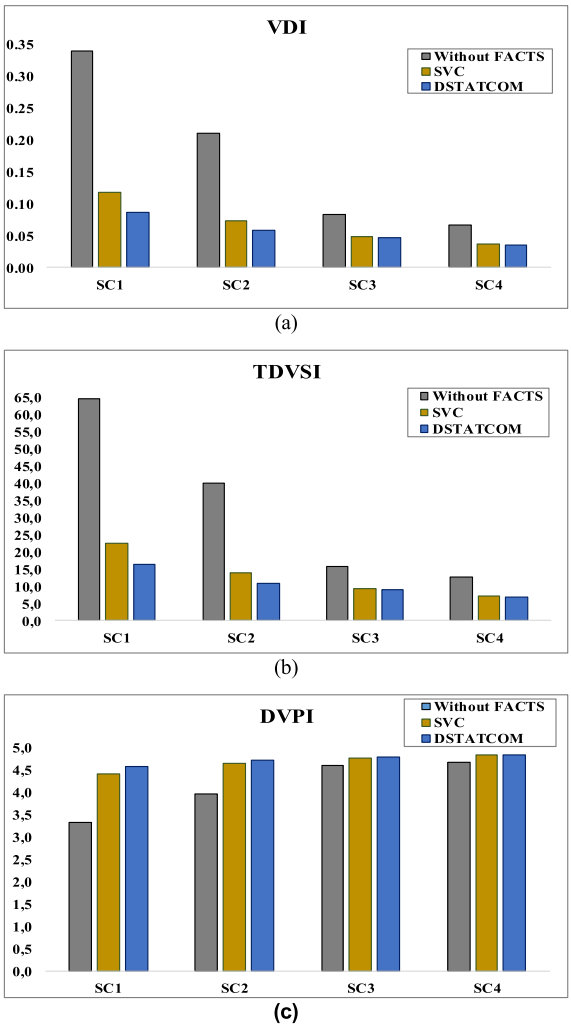

FIGURE 18. Dynamic voltage stability performance indices in the MG with optimal FACTS location: (a) VDI, (b) TDVSI and (c) DVPI.

value of 0.99 p.u. in 0.30 s (1.55 s from the beginning of the simulation). With the DSTATCOM the minimum voltage reached in the perturbation is improved to a value of 0.26 p.u., the temporal response of the voltage is better due to its fast slope reaching 0.98 p.u. in 0.10 s after the MG is isolated and a sustainable stable voltage of 1.00 p.u. in 0.40 s. This allows concluding the operational superiority in the dynamic response of the DSTATCOM device over the SVC, to improve the voltage stability of the isolated MG.

Finally, the results of operating scenario 4 are shown in Fig. 17 (d). It should be noted that this scenario is the one that, to a lesser extent, compromises the dynamic voltage stability, due to the location of the short-circuit that led to the operational isolation of the MG. Additionally, the participation of 30% of the motor dynamic load is also the reason for not witnessing the FIDVR phenomenon, but it was observed a low post-contingency voltage of 0.93 p.u. from 2 s after the start of the simulation process. Namely, during 0.75 s there is a dynamic instability of voltage without oscillations in the signal in the 3 conditions analyzed. Regarding the minimum voltage reached due to the resilient contingencies, it reached a value of 0.35 p.u. In this sense, with the incorporation of SVC and DSTATCOM, the minimum voltages reached were: 0.38 p.u. and 0.45 p.u., respectively. Regarding the post-fault voltage recovery, it is observed that both FACTS devices have a good operating performance, reaching stable permissible voltages of 0.99 p.u. and 1.00 p.u. at 0.10 s and 0.15 s after the contingencies occurred, respectively.

C. COMPARATIVE ANALYSIS BETWEEN SVC AND DSTATCOM DEVICES

The quantitative evaluation indices of the DVS are analyzed to comparatively demonstrate the variability in dynamic operational performance between the two FACTS devices addressed in this research. The results will be exposed for each of the operational scenarios of the MG, taking into account the best locations of the SVC and DSTATCOM obtained in the optimization process of the previous section, and which corresponded to the connection at the PCC node. Thus, the three performance indices: VDI, TDVSI, and DVPI, with their quantitative variabilities, respectively, for the four scenarios assessed are presented in Fig. 18. It should be noted that the respective index without the presence of FACTS has been included in each operational scenario to comparatively visualize the improvements in MG DVS with the incorporation of SVC and DSTATCOM.

Table 8 shows the calculated percentage variations based on the indicated indexes and taking as a reference the individual permissible limits for each one of them, which were expressed in (24) through (26). The results shown highlight the superiority of the DSTATCOM device compared to the SVC in all the scenarios analyzed due to its better operating dynamic response. Additionally, the percentage variation evaluated for the objective function coherent to the optimal location of the two FACTS devices is shown, where it is conclusively shown that the DSTATCOM has contributed in an outstanding way to improve the DVS in the MG in the four operational scenarios.

Once the best location of FACTS was determined, additionally, the improvements achieved in the dynamic performance and reactive power supply of the DERs associated with their respective smart inverters, modeled with the LVRT scheme based on the IEEE-1547-2018 standard, are comparatively shown. For this purpose, the operating state with and without the connection of the FACTS device is taken into consideration and the operating scenario 1 is the one chosen to show the results because this scenario is the most compromised in its dynamic voltage stability. With the

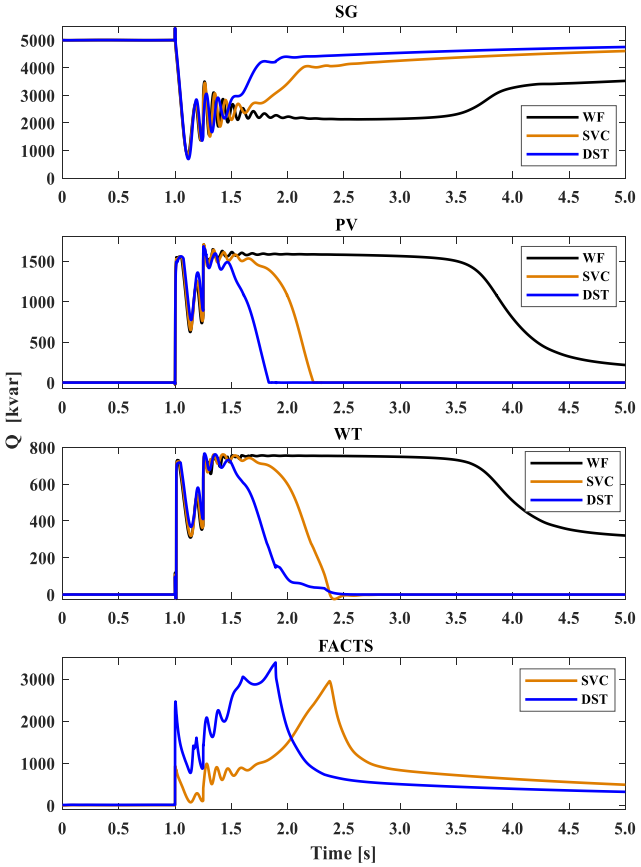

FIGURE 19. Dynamic reactive power performance for each of the DERs without and with the incorporation of FACTS in the MG and dynamic operating performance of SVC and DSTATCOM devices.

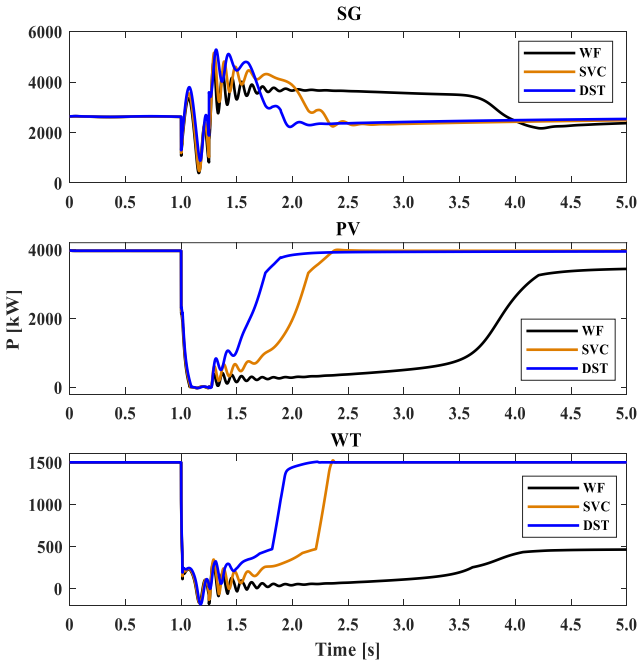

FIGURE 20. Dynamic active power performance for each of the DERs without and with the incorporation of FACTS in the MG.

TABLE 9. Quantitative resilience assessment based on the occurrence of multiple resilient events and operational scenarios.

	Sce $\mathbb{R}$ 1	Sce $\mathbb{R}$ 2	Sce $\mathbb{R}$ 3	Sce $\mathbb{R}$ 4	Sce $\mathbb{R}$ 5	Sce $\mathbb{R}$ 6	Sce $\mathbb{R}$ 7	Sce $\mathbb{R}$ 8
WF	31.87	26.38	17.25	9.92	5.25	2.63	1.26	0.59
SVC	9.29	7.69	5.03	2.89	1.53	0.77	0.37	0.17
DST	6.60	5.46	3.57	2.05	1.09	0.54	0.26	0.12

results shown for this scenario, it is possible to presume a behavior of similar characteristics for the remaining three scenarios, as demonstrated in the previous section. Therefore, the simulations obtained are shown in Fig. 19, where it is demonstrated that the inclusion of FACTS devices produces improvements in the dynamic performance of the reactive power supply for each DER unit of the MG. In this sense, for the synchronous generation (SG), it is observed that in the scenario without FACTS (WF) the output reactive power suffers a sudden drop post-disturbance, which tries to recover after 2.75 s of the occurrence of the contingencies without good results to avoid a dynamic voltage collapse and the presence of FIDVR, due to the absence of sufficient reactive power in the MG. Similarly, for the DERs: PV and WP units, being coupled through smart inverters, operate correctly and efficiently in dynamic support mode of reactive power supply, as shown in the WF scenario. However, this reactive power supply is not entirely enough to improve the DVS of the MG. Nevertheless, with the incorporation of both FACTS, it is shown that after contingencies the reactive power oscillates briefly for a few cycles and recovers efficiently, thus highlighting the better operating performance of the DSTATCOM compared to the SVC. In this sense, it is demonstrated that, with the participation of the SVC and DSTATCOM operating in coordination with the DER units, a correct performance of these inverters in the LVRT scheme can be achieved at the moment of faults and once they are cleared. Thus, the PV and WP reactive power contribution is made while the system is compromised by the contingencies. Consequently, the participation of the FACTS in the dynamic reactive power supply was able to reduce the reactive power stress of the DER inverters and consequently improve the DVS. Complementarily and consequently, with the inclusion of the FACTS devices, a fast and efficient dynamic response of the active power for each of the DERs is achieved, reaching a correct operation of the system, which makes the microgrid operate in a resilient way in its isolation. Fig. 20 shows the dynamic contributions of the active power for each of the DER components of the MG. It is to be noted that, despite the smart type of parameterization in the inverters of these DERs operating in reactive power support mode and without FACTS, an adequate and fast operation of the active power is not achieved. Thus, it is evident that without FACTS the MG could not operate due to supply power problems, which would cause other stability problems in addition to the DVS.

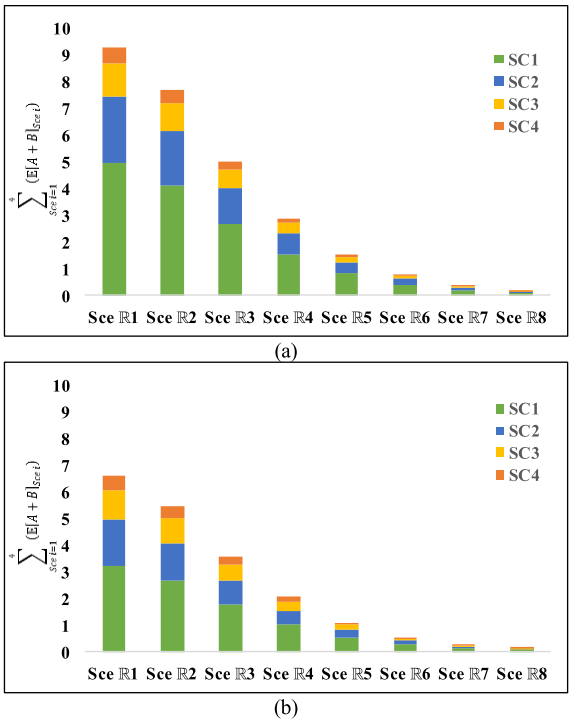

FIGURE 21. Quantitative resilience assessment based on the occurrence of multiple resilient events and operational scenarios for: (a) SVC device and (b) DSTATCOM device.

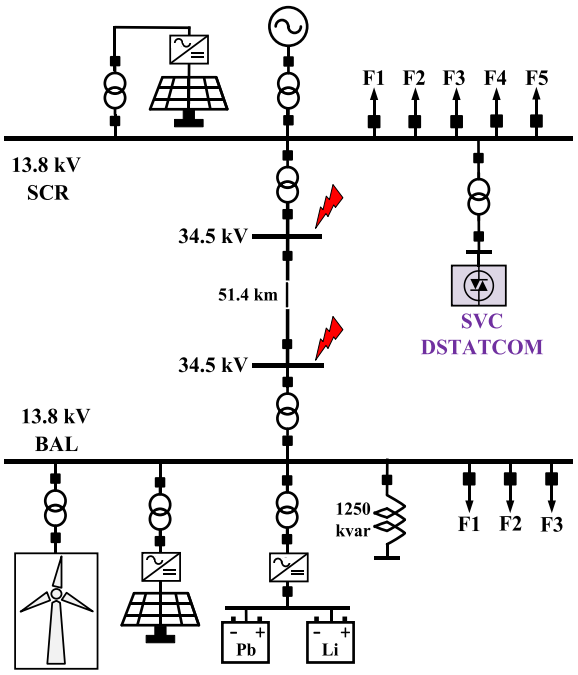

FIGURE 22. Single-line diagram of the Santa Cruz–Baltra microgrid system.

TABLE 10. Santa Cruz – Baltra microgrid generation system.

DERs	*Santa Cruz*	*Baltra*	*Unit*
Photovoltaic	1515	67	kWp
Thermal SG – 1 y 2	6u x 1702	–	kW
Thermal SG – 3	2u x 650	–	kW
Wind power generation	–	3 x 750	kW
Batteries (Pb)	–	4030	kWh
Batteries (Li)	–	270	kWh

Otherwise, to quantify the operational resilience of the MG based on the dynamic performance of the voltage, a mathematical evaluation metric is proposed. The incorporation of an operational resilience evaluation index is considered, which is contingent on a contingency occurrence probability analysis. The index ℝ was previously calculated and exposed in Table 1 and it will be correlated with the four possible operational scenarios considered in the analysis. it is worth noting that, for each resilient scenario (Sce ℝ), it was considered the sum of the expected values calculated according to (11) and accordingly to each of the 4 contingencies based on their operational scenarios (SC). It is necessary to point out that the lower value of this metric means a better level of operational resilience in the MG. Table 9 shows the values obtained for the proposed operational resilience evaluation metric based on dynamic voltage stability performance. The values are presented for the conditions without the incorporation of FACTS and with the incorporation of the two FACTS considered i.e., SVC and DSTATCOM (DST). Conclusively, it is highlighted that DSTATCOM grants better operational resilience to the microgrid in all conditions and scenarios. Nonetheless, the operational performance and contribution of the SVC to improve the dynamic voltage stability and consequently its operational resilience is outstanding in comparison with the operational condition of the MG with no FACTS technology. The results of the resilience evaluation in the MG are graphically presented in Fig. 21 (a) and (b) with the incorporation of both devices (SVC and DSTATCOM). Hence, it is shown that, according to the variability of the historical failure rates, the operational resilience level of the MG varies considerably between each resilient scenario (due to the mathematical Poisson evaluation model). In this sense, the superiority of the DSTATCOM device compared to the SVC is also appreciated. This is due to its better resilience and DVS metrics, as demonstrated in the previous section.

D. TEST SYSTEM 2—GALAPAGOS ISLANDS MICROGRID

The effectiveness of incorporating FACTS in terms of improving the DVS in a test MG has been demonstrated. In this section, the applicability of the previous methodology is extended to a real microgrid with particular operational and topological characteristics. For this study case, a microgrid of the Galapagos Islands in Ecuador is presented. The Galapagos Islands are located 978 km from the Ecuadorian mainland coast. Being geographically and electrically isolated, these islands have their own power generation, transmission, and distribution systems. In particular, the Santa Cruz-Baltra microgrid system is responsible for supplying electricity to the most populated islands. This MG electrically interconnects the islands of Santa Cruz and Baltra, which are

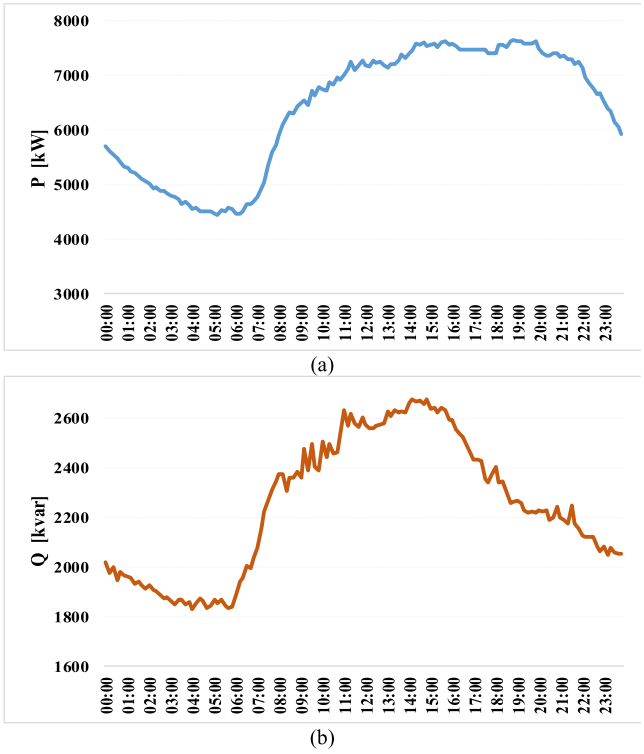

FIGURE 23. Power demand profiles: (a) active and (b) reactive. Maximum demand day microgrid SCR-BAL.

part of the Galapagos archipelago. The single-line diagram of this MG is shown in Fig. 22. This system consists of a sub-transmission line called Santa Cruz-Baltra operating at a rated voltage of 34.5 kV, with a total length of 48.97 km. This line is made up of an overhead grid (19.6 km), an underground submarine cable (21.39 km), and another overhead grid (7.98 km). The generation park is composed of different DERs, and storage systems connected on both islands, which are described below. Santa Cruz has three thermal generation groups and a photovoltaic generation system. On Baltra Island, there are three wind generation units, the Baltra photovoltaic system and a storage system based on lithium-ion and lead acid batteries, details of which are presented in Table 10. Both Santa Cruz and Baltra have 13.8/34.5 kV transformer substations with 10 MVA each. The power distribution system has five and three primary feeders at 13.8 kV for the Santa Cruz and Baltra substations, respectively. In addition, the MG has a 1250 kVAr reactor bank connected to the 13.8 kV system on Baltra Island [64], [65].

Due to the characteristics of the MG's generating park and its particular topology with the interconnection link through the sub-transmission line, several operational problems have arisen, particularly in a dynamic state under the occurrence of disturbances. Among them, the difficulties to maintain voltage stability and reactive power control in this microgrid stand out. This is because the inverters associated with the PV, wind, and battery storage systems are old and, consequently, do not have smart operating characteristics, which allow the supply and dynamic control of reactive power in case of contingencies or voltage dips. Therefore, this work contributes to the modeling and parameterization of the different inverters associated with the DERs, whose operational premises are the smart features based on the IEEE-1547-2018 standard, for dynamic reactive power control and LVRT type operation exposed in section IV. This is with the aim of highlighting that, with the substitution towards new smart inverters, future MG operations can be improved.

1) CHARACTERISTICS OF ELECTRICITY DEMAND IN THE GALAPAGOS ISLANDS

The behavior of the demand for electricity in the Galapagos Islands is seasonal, due to the geographic location of the islands on the Equator (Latitude 0). As a result, the islands have only two climatic seasons: summer (hot season, from November to April) and winter (cold season, from May to October). For the year 2019 (a representative year without COVID-19 pandemic) the annual energy consumed in the Santa Cruz-Baltra microgrid system was 32.5 GWh. The maximum demand in terms of power was reached in the hot summer season, on April 18 (with a maximum temperature around 33°C between 15:00 and 17:30 hours and a relative humidity level of 90%), whose maximum active and reactive power records were 7646 kW and 2676 kVAr, respectively. Regarding the characterization of the demand of the island, it is mainly composed of residential loads. However, due to the massive connection of residential air conditioners that operate throughout the year and to a greater extent in the warm season, difficulties have been evidenced in the supply of reactive power and consequently problems in maintaining voltage control and stability in dynamic and steady-state conditions, motivating the present analysis. The daily demand profiles for active and reactive power taken from the SCADA of the Santa Cruz-Baltra system are graphically shown in Fig. 23 (a) and (b). It should be noted that, in these demand profiles, the power requested from the grid has an increase coinciding with the hours of higher ambient temperature in the islands. Specifically, there is a higher reactive power demand due to the massive use of A/C systems. Therefore, for this operating scenario of maximum hourly demand, different study cases are considered, which will be addressed in the following section.

Due to the geographical and atmospheric conditions of the Galapagos Islands, A/C systems are mostly used for cooling closed environments in homes, hotels, and commercial activities. The A/C type loads respond to dynamic characteristics because they are mainly constituted by induction motors, which lead to difficulties to maintain control and dynamically stabilize the voltage in the MG in the presence of severe contingencies and after they are cleared. In this context, this work also contributes to the modeling and parameterization of this type of dynamic load. This replicates the behavior of the A/C based on the acquired measurements of active and reactive power, obtained through each of the recorders of the primary feeders at 13.8 kV in the Santa Cruz and

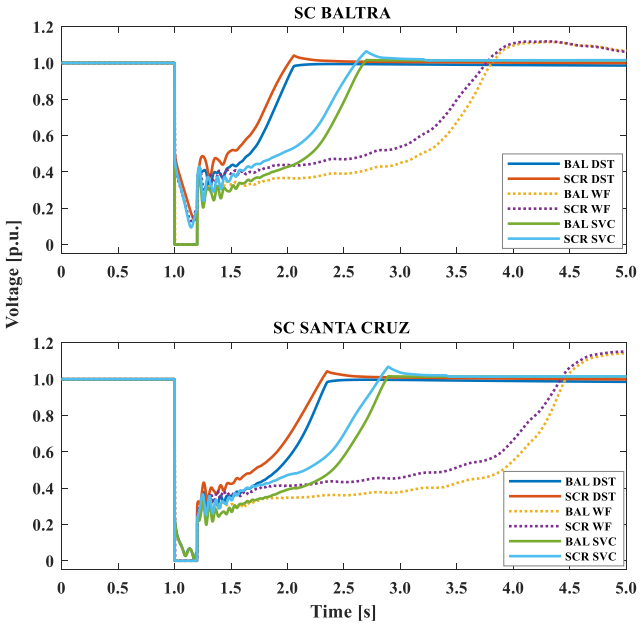

FIGURE 24. Dynamic voltage performance of 34.5 kV buses under short-circuit conditions at Santa Cruz (SCR) and Baltra (BAL) substations.

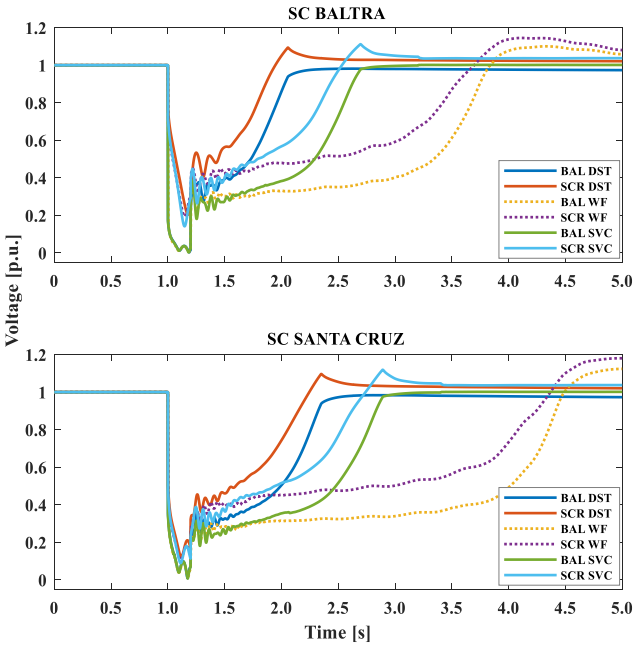

FIGURE 25. Dynamic voltage performance of 13.8 kV busbars under short-circuit conditions at Santa Cruz (SCR) and Baltra (BAL) substations.

Baltra substations, which has been parameterized based on the models previously exposed in section II. For this purpose, it is considered that the percentage participation of the A/C systems corresponds to 70% of the total demand of the MG. That is to say, these A/C models and P-Q type static load were parameterized in each of the primary feeders of Santa Cruz and Baltra substations until reaching the values of active and reactive power recorded in steady-state in the SCADA.

Additionally, it was determined the incorporation of two FACTS technology devices (SVC and DSTATCOM), due to their operational characteristics and results obtained in the previous test MG, improving the dynamic voltage stability. Consequently, the following section will present the different case studies that allow showing the problems in the MG and the way FACTS technology (SVC or DSTATCOM) allow a better operation of the dynamic behavior of the voltage in the Santa Cruz-Baltra system, in the presence of large disturbances.

2) CASE STUDIES

Concerning the present case studies, the occurrence of three-phase transient free-to-ground faults in the 34.5 kV buses of Santa Cruz and Baltra substations, respectively, was considered. This is because these substations are located outdoors and, therefore, are more likely to be affected by faults in areas, where the 34.5 kV buses are opposite the sub-transmission line, which has sections of the underground submarine grid and overhead grid, making the probability of occurrence of faults lower. The faults occur 1 s after the start of the simulation process. The fault detection and clearing time corresponds to 200 ms for each case. Under steady-state conditions, the MG generating park provides the following dispatches P=7850 kW and Q=2720 kVAr, respectively. Regarding the nodal voltages, all of them have a value of 1 p.u. in pre-contingency conditions. Concerning the location of the FACTS devices in this MG, their connection has been determined in the 13.8 kV bus of the Santa Cruz substation, because the highest concentration of system demand is located in this bus.

Subsequently, simulation results for the three cases analyzed are presented: without FACTS and with the connection of devices: SVC and DSTATCOM, respectively. Firstly, the dynamic performances of voltages in p.u. are shown in Fig. 24, as a function of time for the 34.5 kV buses in Baltra (BAL) and Santa Cruz (SCR) substations in the event of the short-circuits (ShC) mentioned in each bus of these substations. It can be seen that, without the incorporation of FACTS and for both short circuits, the dynamic performance of the voltage is seriously compromised, and the appearance of the FIDVR phenomenon. The SCR substation bus is the one most affected by this voltage instability and the late appearance of FIDVR. In addition, in the BAL substation, there is dynamic voltage instability, but the FIDVR phenomenon appears 1 s earlier than in the previous case. The dynamic performances of the voltage with the incorporation of the SVC and DSTATCOM devices are also shown, for both short-circuit situations in each of the buses. The operational superiority of the DSTATCOM is evidenced and demonstrated by dynamically recovering the voltage to its nominal value in less time than the SVC. It is also concluded that both FACTS devices achieved satisfactorily the mitigation of the FIDVR phenomenon.

Subsequently, the results associated with the dynamic voltage performance for the 13.8 kV buses of the Baltra and Santa

TABLE 11. DVPI index microgrid Santa Cruz – Baltra.

Operational Scenario	Without FACTS	SVC	DSTATCOM
SC BAL	3.4995	4.0740	4.3951
SC SCR	3.2631	4.0841	4.5581

TABLE 12. VDI index microgrid Santa Cruz – Baltra.

Operational Scenario	Without FACTS	SVC	DSTATCOM
SC BAL	0.3457	0.2004	0.1390
SC SCR	0.3761	0.2034	0.1231

TABLE 13. TDVSI index microgrid Santa Cruz – Baltra.

Operational Scenario	Without FACTS	SVC	DSTATCOM
SC BAL	113.99	67.11	45.87
SC SCR	124.07	66.08	40.58

Cruz systems is shown in Fig. 25, respectively. In these situations, the differences in dynamic voltage response are shown, determining that in the BAL system, the voltage response is slower compared to the SCR system, since the FACTS were incorporated in the latter system. However, it is shown that at the time of the contingencies the SCR system is the one that most affected its dynamic voltage stability. Comparatively, in terms of speed of response to reach the nominal operating voltage, decrease of oscillations and effective mitigation of FIDVR, it is shown that the DSTATCOM device presents better performance than the SVC. In the analyzed time windows, it was observed that the different nodal voltages of the MG satisfactorily reached the value of 1 p.u. in the post-contingency situation.

Finally, to quantify and comparatively show the differences in the dynamic performance between the SVC and DSTATCOM devices, three tables are shown below with the results obtained for the calculation of the performance indexes related to the dynamic voltage stability applied to the Santa Cruz-Baltra MG system. DVPI, VDI, and TDVSI indices are presented in Tables 11, 12, and 13, respectively, for each of the cases analyzed.

Remarkably, the contingency in the SCR substation bus is the one that most compromise the dynamic voltage performance in the MG. In this sense, it is demonstrated that, with the connection of the FACTS in the 13.8 kV node of the SCR substation, the dynamic voltage stability is enhanced to a greater extent. As in the previous cases, the DSTATCOM is the FACTS device that demonstrates the best dynamic performance against the SVC; this conclusion is supported by the metrics obtained from the indexes. Thus, it is proved that the implementation of FACTS devices in shut connection operating with control schemes coordinated with the distributed generation park allows the improvement of the dynamic voltage stability and consequently, the operational resilience of isolated microgrids in the presence of resilient contingencies and under scenarios of high demand of dynamic loads, such as A/C systems.

VI. DISCUSSION

In this research, it has been determined in the first instance the close relationship between the characterization of the load, including its dynamic and static components, with the phenomena related to voltage instability. Particularly, it was proven that significant shares of dynamic loads such as air conditioning and induction motors (exceeding 50% of the demand component) have a substantial impact on voltage stability and significantly increase the risk of voltage instability in the event of contingencies (short circuit faults) of the resilient type that cause the microgrid to operate isolated. In the same sense, when the distance at which the short circuits occur is closer to the PCC of the MG, it will have a greater effect on compromising the voltage stability of the isolated MG. In contrast, when the contingency is farther away from the PCC it gives more time for the MG to react operationally better in terms of voltage and consequently to be more dynamically stable when the MG is isolated from the distribution system. It should be noted that, in the present research, for the first case study, the participation of renewable generation (PV+WP) based on DERs was higher (67%) compared to the classical generation based on synchronous machines (33%) of the total active power dispatched in the MG. In this context, it could be demonstrated that, the modeling of smart inverters associated with such DERs based on the IEEE-1547-2018 standard guidelines allowed to perform of dynamic reactive power contributions and LVRT support in contingency situations to contribute to minimizing the risk of dynamic voltage collapse. However, it also encountered the problematic difficulty that, when the MG was compromised by the occurrence of simultaneous N-1-1 resilient contingencies even with the reactive power contributions and LVRT response of the smart inverters there were dynamic voltage instabilities that triggered voltage collapses. This situation was very well solved with the incorporation and optimal connection of the SVC and DSTATCOM devices operating in a coordinated manner with the DERs. With respect to operational resilience, the proposed metrics approach constitutes the basis for the analysis and correlation of stability and resilience in microgrids. Particularly, voltage stability was improved with the incorporation of FACTS devices which could be reflected in the improvements in the operational resilience of the MG when it suffers its isolation. Therefore, this research can be considered an innovative initial point in the probabilistic study of operational resilience based on the historical records of occurrences of short-circuit-type contingencies. This allows knowing the response in terms of stability of microgrid systems dominated by DERs coupled to the power grid via electronic power inverters. In this sense, it opens up an interesting research area that can be developed, improved, and approached from different considerations by researchers in the field of microgrids.

On the other hand, regarding the second case study analyzed, it was possible to demonstrate the practical applicability of incorporating FACTS devices in actual microgrid systems such as the case of the Galapagos Islands to improve

the DVS and make up for the reactive power deficit in the event of short-circuit type events. As in the first case study, the superior dynamic performance of the DSTATCOM device over the SVC is highlighted due to the improvement in the DVS of the DSTATCOM device. In this case study, the demand characterization and, consequently the MG load modeling based on SCADA measurements reflected, firstly the validation of the modeling achieved in simulation compared to the actual operation of the Baltra-Santa Cruz MG. Secondly, the modeling of the MG allowed the demonstration of the vulnerability and detriment in the stability of the MG in case of contingencies in its interconnection link between its two subsystems. In this sense, considering the different generation technologies that this MG has, it would be important to consider a hybrid joint operation of storage systems based on batteries and FACTS, specifically, the DSTATCOM to propose improvement alternatives to other stability problems such as frequency and transients. Finally, with the developed methodology it was able to answer the research question of the correlation between DVS and operational resilience, and the way FACTS in MGs can solve these problems in a satisfactory way, which is the main contribution of this work. In addition, it proposes a new area of research in MGs, which will generate opportunities for analysis and discussion.

VII. CONCLUSION

In this paper, the impact of including shunt-connected FACTS devices in order to improve the dynamic voltage stability in resilient microgrids has been analyzed and investigated. The different case studies and scenarios considered were carried out in a reference test MG system and in the actual microgrid system of the Galapagos Islands in Ecuador. The results obtained revealed that a high penetration of dynamic loads of IM and A/C types in MG systems mainly cause the presence of the FIDVR phenomenon, dynamic instabilities, and rapid voltage collapses when resilient contingencies occur. An additional aspect to emphasize is that the location of the short circuits in their proximity to the MG PCC or load centers also have a substantial impact in compromising the DVS. These operational situations are worsened in the absence of smart inverters that provide dynamic reactive power support and LVRT-type control schemes. Nevertheless, it was demonstrated that, with a control scheme for solar PV and wind DER inverters, based on the IEEE-1547-2018 standard operating in coordination with the FACTS either SVC or DSTATCOM, significant improvements in performance and dynamic voltage stability are obtained even mitigating completely the FIDVR in all scenarios and circumstances analyzed. Regarding the determination of the optimal nodal location in the connection of the FACTS in the MG, the different resilient contingencies in the feeders and interconnection link to the grid were considered. A mixed integer optimization problem developed in Python (Pyomo) was formulated based on the performance indexes calculated from the voltage vs. time signals obtained in the simulation stage via PowerFactory. This achieves an optimization strategy of easy implementation and with results attached to the objective of improving the DVS in the MG. However, for the Galapagos MG system, only the occurrence of contingencies in the buses of the two MG subsystems was considered, the worst operating condition was analyzed, and it was determined that the best nodal location for the connection of the FACTS corresponded to the load center bus; thus improving the dynamic voltage stability in all MG nodes. In terms of comparative response and operational performance, the DSTATCOM device presented greater improvements in dynamic voltage stability in the two MG systems addressed than its peer the SVC. Finally, the proposal of quantitative evaluation metrics of resilient contingencies allowed to contribute with a mathematical model that identifies the vulnerability of the MG to the detriment of its resilience according to statistics of its disturbances, as well as the improvements achieved with the incorporation of FACTS devices operating in coordination with the DERs. Future advances to the topic developed in this research should be focused on the use of other types of FACTS technology devices and controllers to improve the stability in terms of frequency and voltage, as well as the power quality of isolated microgrids. Additionally, new metrics and indexes should be proposed to address the analysis of the operational resilience of microgrid systems. Finally, another important aspect that would contribute to the results that we have exposed would be to reproduce the proposed methodology and embedded case studies through hardware-in-the-loop tools.

REFERENCES

[1] S. Parhizi, H. Lotfi, A. Khodaei, and S. Bahramirad, "State of the art in research on microgrids: A review," *IEEE Access*, vol. 3, pp. 890–925, 2015, doi: 10.1109/ACCESS.2015.2443119.

[2] F. Martin-Martínez, A. Sánchez-Miralles, and M. Rivier, "A literature review of microgrids: A functional layer based classification," *Renew. Sustain. Energy Rev.*, vol. 62, pp. 1133–1153, Sep. 2016, doi: 10.1016/j.rser.2016.05.025.

[3] N. M. Tabatabaei, E. Kabalci, and N. Bizon, *Microgrid Architectures, Control and Protection Methods*. Cham, Switzerland: Springer, 2020, doi: 10.1007/978-3-030-23723-3.

[4] A. A. Eajal, A. H. Yazdavar, E. F. El-Saadany, and K. Ponnambalam, "On the loadability and voltage stability of islanded AC–DC hybrid microgrids during contingencies," *IEEE Syst. J.*, vol. 13, no. 4, pp. 4248–4259, Dec. 2019, doi: 10.1109/JSYST.2019.2910734.

[5] S. Adhikari, J. Schoene, N. Gurung, and A. Mogilevsky, "Fault induced delayed voltage recovery (FIDVR): Modeling and guidelines," in *Proc. IEEE Power Energy Soc. Gen. Meeting (PESGM)*, Aug. 2019, pp. 1–5, doi: 10.1109/PESGM40551.2019.8973440.

[6] E. Hajipour, H. Saber, N. Farzin, M. R. Karimi, S. M. Hashemi, A. Agheli, H. Ayoubzadeh, and M. Ehsan, "An improved aggregated model of residential air conditioners for FIDVR studies," *IEEE Trans. Power Syst.*, vol. 35, no. 2, pp. 909–919, Mar. 2020, doi: 10.1109/TPWRS.2019.2940596.

[7] J. D. R. Penaloza, J. A. Adu, A. Borghetti, F. Napolitano, F. Tossani, and C. A. Nucci, "Influence of load dynamic response on the stability of microgrids during islanding transition," *Electric Power Syst. Res.*, vol. 190, Jan. 2021, Art. no. 106607, doi: 10.1016/j.epsr.2020.106607.

[8] M. Islam, N. Mithulananthan, and M. J. Hossain, "Dynamic voltage support by TL-PV systems to mitigate short-term voltage instability in residential DN," *IEEE Trans. Power Syst.*, vol. 33, no. 4, pp. 4360–4370, Jul. 2018, doi: 10.1109/TPWRS.2017.2765311.

[9] L. Lin, X. Zhao, J. Zhu, X. Zhang, and R. Yang, "Simulation analysis of microgrid voltage stability with multi-induction motor loads," *Electric Power Compon. Syst.*, vol. 46, no. 5, pp. 560–569, Mar. 2018, doi: 10.1080/15325008.2018.1459958.

[10] J. Schiffer, T. Seel, J. Raisch, and T. Sezi, "Voltage stability and reactive power sharing in inverter-based microgrids with consensus-based distributed voltage control," *IEEE Trans. Control Syst. Technol.*, vol. 24, no. 1, pp. 96–109, Jan. 2016, doi: 10.1109/TCST.2015.2420622.

[11] T. Khamkhong, B. Sookananta, and M. Pusayatanont, "Dynamic voltage support using PV inverter to mitigate short-term voltage stability of microgrid," in *Proc. Int. Conf. Power, Energy Innov. (ICPEI)*, Oct. 2021, pp. 65–68, doi: 10.1109/ICPEI52436.2021.9690660.

[12] L. A. Paredes, M. G. Molina, and B. R. Serrano, "Resilient microgrids with FACTS technology," in *Proc. IEEE PES Transmiss. Distrib. Conf. Exhib.-Latin Amer. (T&D LA)*, Montevideo, Uruguay, Sep./Oct. 2020, pp. 1–6, doi: 10.1109/TDLA47668.2020.9326097.

[13] T. Samad and A. M. Annaswamy, "Controls for smart grids: Architectures and applications," *Proc. IEEE*, vol. 105, no. 11, pp. 2244–2261, Nov. 2017, doi: 10.1109/JPROC.2017.2707326.

[14] L. A. Paredes, B. R. Serrano, and M. G. Molina, "FACTS technology to improve the operation of resilient microgrids," in *Proc. FISE-IEEE/CIGRE Conf.-Living Energy Transition*, Medellin, Colombia, Dec. 2019, pp. 1–7, doi: 10.1109/FISECIGRE48012.2019.8984960.

[15] A. H. Al-Mubarak, S. M. Bamsak, B. Thorvaldsson, M. Halonen, and R. Grunbaum, "Preventing voltage collapse by large SVCs at power system faults," in *Proc. IEEE/PES Power Syst. Conf. Expo.*, Mar. 2009, pp. 1–9, doi: 10.1109/PSCE.2009.4840189.

[16] M. Paramasivam, A. Salloum, V. Ajjarapu, V. Vittal, N. B. Bhatt, and S. Liu, "Dynamic optimization based reactive power planning to mitigate slow voltage recovery and short term voltage instability," *IEEE Trans. Power Syst.*, vol. 28, no. 4, pp. 3865–3873, Nov. 2013, doi: 10.1109/TPWRS.2013.2271260.

[17] R. K. Varma and S. Mohan, "Mitigation of fault induced delayed voltage recovery (FIDVR) by PV-STATCOM," *IEEE Trans. Power Syst.*, vol. 35, no. 6, pp. 4251–4262, Nov. 2020, doi: 10.1109/TPWRS.2020.2991447.

[18] J. Qi, W. Zhao, and X. Bian, "Comparative study of SVC and STATCOM reactive power compensation for prosumer microgrids with DFIG-based wind farm integration," *IEEE Access*, vol. 8, pp. 209878–209885, 2020, doi: 10.1109/ACCESS.2020.3033058.

[19] T. Aziz, U. P. Mhaskar, T. K. Saha, and N. Mithulananthan, "An index for STATCOM placement to facilitate grid integration of DER," *IEEE Trans. Sustain. Energy*, vol. 4, no. 2, pp. 451–460, Apr. 2013, doi: 10.1109/TSTE.2012.2227517.

[20] A. H. Elmetwaly, A. A. Eldesouky, and A. A. Sallam, "An adaptive D-FACTS for power quality enhancement in an isolated microgrid," *IEEE Access*, vol. 8, pp. 57923–57942, 2020, doi: 10.1109/ACCESS.2020.2981444.

[21] A. Hamidi, S. Golshannavaz, and D. Nazarpour, "D-FACTS cooperation in renewable integrated microgrids: A linear multiobjective approach," *IEEE Trans. Sustain. Energy*, vol. 10, no. 1, pp. 355–363, Jan. 2019, doi: 10.1109/TSTE.2017.2723163.

[22] Q. Wang, B. Wang, W. Xu, and J. Xu, "Research on STATCOM for reactive power flow control and voltage stability in microgrid," in *Proc. 13th IEEE Conf. Ind. Electron. Appl. (ICIEA)*, May 2018, Art. no. 61671338, doi: 10.1109/ICIEA.2018.8398126.

[23] R. M. M. Pereira, A. J. C. Pereira, C. M. M. Ferreira, and F. P. M. Barbosa, "STATCOM to improve the voltage stability of an electric power system with high penetration of wind generation," in *Proc. 51st Int. Universities Power Eng. Conf. (UPEC)*, Sep. 2016, pp. 1–5, doi: 10.1109/UPEC.2016.8114142.

[24] L. A. Paredes, M. G. Molina, and B. R. Serrano, "Improvement of dynamic voltage stability in a microgrid using a DSTATCOM," *Revista Iberoamericana de Automática e Informática Ind.*, vol. 18, no. 4, pp. 385–395, 2021, doi: https://doi.org/10.4995/riai.2021.14813.

[25] A. V. Jayawardena, L. G. Meegahapola, D. A. Robinson, and S. Perera, "Low-voltage ride-through characteristics of microgrids with distribution static synchronous compensator (DSTATCOM)," in *Proc. Australas. Universities Power Eng. Conf. (AUPEC)*, Sep. 2015, pp. 1–6, doi: 10.1109/AUPEC.2015.7324823.

[26] W. Wang and F. de León, "Quantitative evaluation of DER smart inverters for the mitigation of FIDVR in distribution systems," *IEEE Trans. Power Del.*, vol. 35, no. 1, pp. 420–429, Feb. 2020, doi: 10.1109/TPWRD.2019.2929547.

[27] N. Afrin, F. Yang, and J. Lu, "Optimized reactive power support strategy for photovoltaic inverter to intensify the dynamic voltage stability of islanded microgrid," *Int. Trans. Electr. Energy Syst.*, vol. 30, no. 6, pp. 1–16, Jun. 2020, doi: 10.1002/2050-7038.12356.

[28] G. Fernández, A. Martínez, N. Galán, J. Ballestín-Fuertes, J. Muñoz-Cruzado-Alba, P. López, S. Stukelj, E. Daridou, A. Rezzonico, and D. Ioannidis, "Optimal D-STATCOM placement tool for low voltage grids," *Energies*, vol. 14, no. 14, p. 4212, Jul. 2021, doi: 10.3390/en14144212.

[29] S. Ranjan, D. C. Das, N. Sinha, A. Latif, S. M. S. Hussain, and T. S. Ustun, "Voltage stability assessment of isolated hybrid dish-stirling solar thermal-diesel microgrid with STATCOM using mine blast algorithm," *Electr. Power Syst. Res.*, vol. 196, Jul. 2021, Art. no. 107239, doi: 10.1016/J.EPSR.2021.107239.

[30] L. Elkhidir, K. Khan, M. Al-Muhaini, and M. Khalid, "Enhancing transient response and voltage stability of renewable integrated microgrids," *Sustainability*, vol. 14, no. 7, pp. 1–21, 2022, doi: 10.3390/su14073710.

[31] S. Chakraborty, S. Mukhopadhyay, and S. K. Biswas, "Coordination of D-STATCOM & SVC for dynamic VAR compensation and voltage stabilization of an AC grid interconnected to a DC microgrid," *IEEE Trans. Ind. Appl.*, vol. 58, no. 1, pp. 634–644, Jan. 2022, doi: 10.1109/TIA.2021.3123264.

[32] A. A. Nafeh, A. Heikal, R. A. El-Sehiemy, and W. A. A. Salem, "Intelligent fuzzy-based controllers for voltage stability enhancement of AC–DC micro-grid with D-STATCOM," *Alexandria Eng. J.*, vol. 61, no. 3, pp. 2260–2293, Mar. 2022, doi: 10.1016/j.aej.2021.07.012.

[33] F. Chang, J. O'Donnell, and W. Su, "Voltage stability assessment of AC/DC hybrid microgrid," *Energies*, vol. 16, no. 1, p. 399, Dec. 2022, doi: 10.3390/en16010399.

[34] H. M. El Zoghby and H. S. Ramadan, "Isolated microgrid stability reinforcement using optimally controlled STATCOM," *Sustain. Energy Technol. Assessments*, vol. 50, Mar. 2022, Art. no. 101883, doi: 10.1016/j.seta.2021.101883.

[35] A. M. Nakiganda, T. van Cutsem, and P. Aristidou, "Microgrid operational optimization with dynamic voltage security constraints," in *Proc. IEEE Madrid PowerTech*, Jun. 2021, pp. 1–6, doi: 10.1109/PowerTech46648.2021.9494823.

[36] A. M. Nakiganda and P. Aristidou, "Resilient microgrid scheduling with secure frequency and voltage transient response," *IEEE Trans. Power Syst.*, vol. 38, no. 4, pp. 3580–3592, Jul. 2023, doi: 10.1109/TPWRS.2022.3207523.

[37] K. Singh, M. Amir, F. Ahmad, and S. S. Refaat, "Enhancement of frequency control for stand-alone multi-microgrids," *IEEE Access*, vol. 9, pp. 79128–79142, 2021, doi: 10.1109/ACCESS.2021.3083960.

[38] Zaheeruddin, K. Singh, and M. Amir, "Intelligent fuzzy TIDF-II controller for load frequency control in hybrid energy system," *IETE Tech. Rev.*, vol. 39, no. 6, pp. 1355–1371, Nov. 2021, doi: 10.1080/02564602.2021.1994476.

[39] M. Amir, A. K. Prajapati, and S. S. Refaat, "Dynamic performance evaluation of grid-connected hybrid renewable energy-based power generation for stability and power quality enhancement in smart grid," *Frontiers Energy Res.*, vol. 10, pp. 1–16, Mar. 2022, doi: 10.3389/fenrg.2022.861282.

[40] M. N. Alam, S. Chakrabarti, and X. Liang, "A benchmark test system for networked microgrids," *IEEE Trans. Ind. Informat.*, vol. 16, no. 10, pp. 6217–6230, Oct. 2020, doi: 10.1109/TII.2020.2976893.

[41] N. Hosseinzadeh, A. Aziz, A. Mahmud, A. Gargoom, and M. Rabbani, "Voltage stability of power systems with renewable-energy inverter-based generators: A review," *Electronics*, vol. 10, no. 2, p. 115, Dec. 2021, doi: 10.3390/electronics10020115.

[42] M. Farrokhabadi, C. A. Canizares, J. W. Simpson-Porco, E. Nasr, L. Fan, P. A. Mendoza-Araya, R. Tonkoski, U. Tamrakar, N. Hatziargyriou, D. Lagos, and R. W. Wies, "Microgrid stability definitions, analysis, and examples," *IEEE Trans. Power Syst.*, vol. 35, no. 1, pp. 13–29, Jan. 2020, doi: 10.1109/TPWRS.2019.2925703.

[43] J. M. Guerrero, M. Chandorkar, T. Lee, and P. C. Loh, "Advanced control architectures for intelligent microgrids—Part I: Decentralized and hierarchical control," *IEEE Trans. Ind. Electron.*, vol. 60, no. 4, pp. 1254–1262, Apr. 2013, doi: 10.1109/TIE.2012.2194969.

[44] Y. Xu, Z. Y. Dong, K. Meng, W. F. Yao, R. Zhang, and K. P. Wong, "Multi-objective dynamic VAR planning against short-term voltage instability using a decomposition-based evolutionary algorithm," *IEEE Trans. Power Syst.*, vol. 29, no. 6, pp. 2813–2822, Nov. 2014, doi: 10.1109/TPWRS.2014.2310733.

[45] J. Shi, L. Ma, C. Li, N. Liu, and J. Zhang, "A comprehensive review of standards for distributed energy resource grid-integration and microgrid," *Renew. Sustain. Energy Rev.*, vol. 170, Dec. 2022, Art. no. 112957, doi: 10.1016/j.rser.2022.112957.

[46] H. A. Villarroel-Gutiérrez and M. Molina, "Analysis of dynamic voltage support schemes for PV generators implemented in Latin America," *IEEE Latin Amer. Trans.*, vol. 18, no. 4, pp. 641–651, Apr. 2020, doi: 10.1109/TLA.2020.9082206.
[47] *Standard for Interconnection and Interoperability of Distributed Energy Resources With Associated Electric Power Systems Interfaces*, IEEE Standard 1547-2018, 2018.
[48] K. Padiyar and A. M. Kulkarni, *Dynamics and Control of Electric Transmission and Microgrids*, vol. 21. Hoboken, NJ, USA: Wiley, Dec. 2018, doi: 10.1002/9781119173410.
[49] G. Lo Giudice, G. D. Amico, and F. Gallego, "Análisis de Fenómenos de Colapso de Tensión Mediante el uso de nuevos modelos para Aires Acondicionados," in *Décimo Quinto Encuentro Regional Ibero-americano del CIGRÉ*. Foz do Iguaçu, Brazil: XV ERIAC, 2013, pp. 1–8.
[50] *PowerFactory Technical User Manual*, DIgSILENT, Gomaringen, Germany, 2018.
[51] T. A. Alaqeel, S. A. Almohaimeed, and S. Suryanarayanan, "A review of air conditioning motor loads stalling on voltage recovery in the Saudi electric grid," in *Proc. North Amer. Power Symp. (NAPS)*, Morgantown, WV, USA, Sep. 2017, pp. 1–6, doi: 10.1109/NAPS.2017.8107175.
[52] R. J. Bravo, R. Yinger, and P. Arons, "Fault induced delayed voltage recovery (FIDVR) indicators," in *Proc. IEEE PES T&D Conf. Expo.*, Apr. 2014, pp. 1–5, doi: 10.1109/TDC.2014.6863324.
[53] S. V. Kolluri, J. R. Ramamurthy, S. M. Wong, M. Peterson, P. Yu, and M. R. Chander, "Relay-based undervoltage load shedding scheme for Entergy's Western Region," in *Proc. IEEE Power Energy Soc. Gen. Meeting*, Jul. 2015, pp. 4–8, doi: 10.1109/PESGM.2015.7285651.
[54] Y. Du, Q. Huang, R. Huang, T. Yin, J. Tan, W. Yu, and X. Li, "Physics-informed evolutionary strategy based control for mitigating delayed voltage recovery," *IEEE Trans. Power Syst.*, vol. 37, no. 5, pp. 3516–3527, Sep. 2022, doi: 10.1109/TPWRS.2021.3132328.
[55] H. Saber, M. R. Karimi, E. Hajipour, N. Farzin, S. M. Hashemi, A. Agheli, H. Ayoubzadeh, and M. Ehsan, "Investigating the effect of ambient temperature on fault-induced delayed voltage recovery events," *IET Gener., Transmiss. Distrib.*, vol. 14, no. 9, pp. 1781–1790, May 2020, doi: 10.1049/iet-gtd.2019.1025.
[56] R. Bekhradian, M. Sanaye-Pasand, and M. Davarpanah, "Innovative load shedding scheme to restore synchronous generator-based microgrids during FIDVR," *IEEE Trans. Smart Grid*, vol. 14, no. 1, pp. 388–399, Jan. 2023, doi: 10.1109/TSG.2022.3190002.
[57] A. R. R. Matavalam, R. Venkatraman, and V. Ajjarapu, "Mitigating delayed voltage recovery using DER & load control in distribution systems," in *Proc. IEEE Power Energy Soc. Gen. Meeting (PESGM)*, Denver, CO, USA, Jul. 2022, pp. 1–5, doi: 10.1109/PESGM48719.2022.9916669.
[58] B. W. Tuinema, J. L. Rueda Torres, A. I. Stefanov, F. M. Gonzalez-Longatt, and M. A. M. M. van der Meijden, *Probability Reliability Analysis of Power Systems A Student's Introduction*. Cham, Switzerland: Springer, 2020.
[59] N. Tleis. (2019). *Power Systems Modelling and Fault Analysis*. [Online]. Available: http://library1.nida.ac.th/termpaper6/sd/2554/19755.pdf
[60] L. A. Paredes, M. G. Molina, and B. R. Serrano, "Improvements in the voltage stability of a microgrid due to smart FACTS—An approach from resilience," in *Proc. IEEE ANDESCON*, Oct. 2020, pp. 1–6.
[61] J. J. Shea, "Understanding FACTS-concepts and technology of flexible AC transmission systems [book review]," *IEEE Elect. Insul. Mag.*, vol. 18, no. 1, p. 46, Jan. 2002, doi: 10.1109/mei.2002.981326.
[62] M. Molina and P. Mercado, "Control design and simulation of DSTATCOM with energy storage for power quality improvements," in *Proc. IEEE/PES Transmiss. Distrib. Conf. Expo., Latin Amer.*, Aug. 2006, pp. 1–7, doi: 10.1109/TDCLA.2006.311436.
[63] W. E. Hart, C. Laird, J.-P. Watson, and D. L. Woodruff, *Pyomo—Optimization Modeling in Python*, vol. 67, 3rd ed. Cham, Switzerland: Springer, 2021, doi: https://doi.org/10.1007/978-3-030-68928-5.
[64] L. A. Paredes, M. G. Molina, and B. R. Serrano, "Enhancing the voltage stability of a galapagos microgrid using a DSTATCOM," in *Proc. IEEE Congreso Bienal de Argentina (ARGENCON)*, Dec. 2020, pp. 1–7, doi: 10.1109/ARGENCON49523.2020.9505450.
[65] A. A. Eras-Almeida, M. A. Egido-Aguilera, P. Blechinger, S. Berendes, E. Caamaño, and E. García-Alcalde, "Decarbonizing the Galapagos islands: Techno-economic perspectives for the hybrid renewable minigrid Baltra–Santa Cruz," *Sustainability*, vol. 12, pp. 1–48, Mar. 2020, doi: 10.3390/su12062282.

LUIS A. PAREDES (Member, IEEE) was born in Quito, Ecuador, in 1987. He received the B.S. degree in electrical engineering and the M.Sc. degree in energy management from Escuela Politécnica Nacional, Ecuador, in 2012 and 2016, respectively, and the Diploma degree in electromobility from Universidad de Santiago de Chile, Chile, in 2021. He is currently pursuing the Ph.D. degree in electrical engineering with Instituto de Energía Eléctrica (IEE), Universidad Nacional de San Juan (UNSJ), Argentina. His current research interests include stability and control in electric microgrids, FACTS, the resilience of electric systems, electromobility, renewable energies, and energy efficiency.

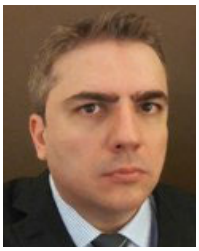

MARCELO G. MOLINA (Senior Member, IEEE) received the Electronic Engineering and Ph.D. degrees from Universidad Nacional de San Juan (UNSJ), in 1997 and 2004, respectively. In 2004, he was a Doctoral Research Fellow with Universidad Federal de Rio de Janeiro (UFRJ), Brazil. From 2005 to 2007, he was a Postdoctoral Research Fellow with the National Scientific and Technical Research Council (CONICET), Instituto de Energía Eléctrica (IEE). In 2009, he was a Visiting Professor with Universität Siegen, Germany, and UFRJ, in 2010. From 2010 to 2018, he was the Vice-Director of IEE. Since 2019, he has been the Director of the Faculty of Engineering, IEE, UNSJ-CONICET. He is currently a Full Professor of electrical engineering with the Faculty of Engineering, UNSJ, and a Senior Researcher with CONICET, Argentina, where he also holds various academic and executive positions. He is also a Senior Power Systems Engineering Consultant with IEE, where he is providing services in a variety of market sectors. In all these positions, he had extensive research, teaching, speaking, and executive experience in numerous power engineering areas. He has been involved in many national and international projects and high-level power systems consulting with government agencies and companies. He has collaborated with industry and university researchers in Argentina and abroad, and supervising/co-supervising many research fellows and graduate students. His current research interests include power system modeling, analysis and control, power electronics and electrical drives, microgrid and smart grid technologies, renewable generation, and energy storage.

BENJAMÍN R. SERRANO was born in San Juan, Argentina, in 1955. He received the degree in electromechanical engineering from Universidad Nacional de San Juan (UNSJ), Argentina, and the Ph.D. degree in electrical engineering from Instituto de Energía Eléctrica (IEE), UNSJ, in 2017. Since 2020, he has been the Vice-Director of IEE, UNSJ. His current research interests include the optimal programming of the operation of electrical power systems, considering voltage control, and reactive power supply.